

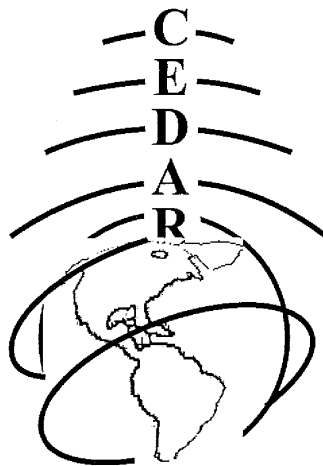
CEDAR 2014

Cascade Ballroom, Haggett Hall
University of Washington



Seattle, Washington

IT Poster Session
Tuesday June 24, 2014



"CEDAR Grand Challenges"

Table of Contents

Data Assimilation or Management

DATA-01	Gary Steven Bust, A Data Assimilative Comparison of Solar Cycle 24 Magnetic Storms.....	1
DATA-02	Brian J. Harding, Data fusion from a network of Fabry-Perot interferometers: Estimation of regional thermospheric wind dynamics.....	1
DATA-03	Chih Ting Hsu Effects of estimating unobserved thermosphere-ionosphere states by data assimilation of FORMOSAT-3/COSMIC data on global ionospheric forecasting.....	1
DATA-04	Chi-Yen Lin, Ionospheric Assimilation of Radio Occultation and Ground-based GPS data using Non-stationary Background Model Error Covariance.....	2
DATA-05	Romina Nikoukar, Specification of the plasmasphere using a new data assimilation approach.....	3
DATA-06	Dave Pawlowski, Using Ensemble Simulations to Assess Uncertainty in the Upper Atmosphere.....	3
DATA-07	Yang-Yi Sun, Assimilative Neutral Wind Bias Correction Scheme for Global Ionospheric Modeling at Midlatitude.....	3

Equatorial Thermosphere or Ionosphere

EQIT-01	Juan C. Espinoza, LISN network: TEC observations over South America.....	4
EQIT-02	Marc Hairston, The equatorial ionosphere's response to the October 2012 geomagnetic storms.....	4
EQIT-03	Ehab Hassan, Equatorial Electrojet Irregularities- New Fluid Approach and Simulation.....	5
EQIT-04	Dustin A. Hickey, Boston University All-Sky Imager at the Jicamarca Radio Observatory.....	5
EQIT-05	Junseok Hong, Equinoctial asymmetry of transition heights in topside ionospheric profiles.....	5
EQIT-06	Andrew Devon Kiene, Westward neutral winds in the postsunset equatorial Thermosphere.....	6
EQIT-07	Vicki Hsu, Altitude Structure of the Equatorial Thermosphere Anomaly.....	6
EQIT-08	Rebecca MacInnis, Zonal drifts from all-sky imaging observations and CINDI data: magnetically conjugate behavior and latitudinal shear.....	7

EQIT-09	Cesar Enrique Valladares, The Tropical Ionization Anomaly	7
EQIT-10	Juliano Moro, Equatorial Electric Fields in the Brazilian and Peruvian Sectors.....	7
EQIT-11	Edgardo Pacheco, Observations of low-latitude irregularities during low and moderate solar activity.....	8
EQIT-12	Fabiano Rodrigues, MELISSA: A new coherent backscatter radar interferometer for the Brazilian sector	8
EQIT-13	Jessica Mae Smith, On the magnitude of equatorial pre-reversal enhancement of the ionospheric zonal electric field and equatorial topside irregularities.....	9
EQIT-14	Robert Michael Sorbello, First steps towards the implementation of a cognitive radar to study plasma instabilities near the Peruvian Andes	9
EQIT-15	Daniel Suarez Munoz, Signal Chain Software for Jicamarca Radar.....	10

Instruments or Techniques for Ionospheric or Thermospheric Observation

ITIT-01	Carl Andersen, Measurement of Neutral Winds and Gradients in the Lower Thermosphere with Multi-Point, Chemical-Release Sounding Rocket Payloads	10
ITIT-02	Manbharat Singh Dhadly, First ever cross-comparison of thermospheric neutral wind measured by narrow and wide field optical Doppler spectroscopy.....	11
ITIT-03	Philip Fernandes, Possible measurements of low-altitude ion conics from the MICA sounding rocket.....	11
ITIT-04	Derek Gardner, First Balmer-a Airglow Temperature Observations using Field-Widened Spatial Heterodyne Spectroscopy	12
ITIT-05	George R. Geddes, Ionospheric Inversion Using OII 83.4 nm Observations.....	12
ITIT-06	Chhavi Goenka, Versatile four channel tunable hyperspectral imager for remote sensing.....	13
ITIT-07	Monica Hew, Optical Characterization Methods for Assessing Threat of Spacecraft Electrical Anomaly due to Hypervelocity Impact Plasma	13
ITIT-08	Karim M. Kuyeng Ruiz, Preliminary results of the PSU All-sky Radar Interferometry System (PARIS).....	13
ITIT-10	Michelle Lynn Pyle, Design for Miniaturized Time-of-Flight Reflectron Mass Spectrometer for Upper Atmosphere Density Measurements.....	14
ITIT-11	Ashton Seth Reimer, Estimation of Self-Clutter for HF Ionospheric Radars that Employ the Multi-pulse Technique	14
ITIT-12	Ashton Seth Reimer, Determination of an Optimal Pulse-Repetition Time for SuperDARN radars.....	15

ITIT-13	Weiwei Sun, High speed multi-antenna radar receiver.....	15
ITIT-14	John P. Swoboda, Plasma Motion Induced Artifacts in 3-D Incoherent Scatter Radar.....	15
ITIT-15	Nicole Tatton, The Optical Profiling of the Atmospheric Limb (OPAL) CubeSat Experiment.....	16

Irregularities of Ionosphere or Atmosphere

IRRI-01	Shih-Ping Chen, Occultation Scintillation Observed by FORMOSAT-3/COSMIC in 2007-2014.....	17
IRRI-02	Russell Bonner Cosgrove, Alfvén waves in the ionosphere: cutoff altitude and feedback instability.....	17
IRRI-03	Geoff Crowley, Acoustic Waves Detected in the F-region Ionosphere by the TIDDBIT HF TID Mapping System.....	17
IRRI-04	Geoff Crowley, TID Observations at Middle and Low Latitudes Using the TIDDBIT HF TID Mapper.....	18
IRRI-05	Geoff Crowley, OSSE Experiments to Determine the Value of Various Observing Systems for Ionosphere-Thermosphere Specification.....	18
IRRI-06	Kshitija Bharat Deshpande, Inverse modeling using a novel GPS scintillation model, SIGMA, to characterize high latitude irregularities.....	19
IRRI-07	Ahmed Said Hassan Eltrass, Identification of the generation source of decameter-scale ionospheric irregularities on plasmopause field lines.....	20
IRRI-08	Leslie Jean Lamarche, A statistical investigation of decameter-scale plasma waves in the polar F region.....	20
IRRI-09	Fei-Fan Lin, Observations of three dimensional spatial plasma structures of F region 3-m field-aligned irregularities made with Chung-Li VHF radar.....	21
IRRI-10	Christer van der Meeren, GNSS scintillations in the nightside polar ionosphere over Svalbard.....	21
IRRI-11	Chien-Ya Wang, Characteristics of 3-m field-aligned irregularities in daytime and nighttime sporadic E region made with Chung-Li VHF radar.....	22
IRRI-12	Tatsuhiko Yokoyama, Three-dimensional high-resolution plasma bubble modeling.....	22
IRRI-13	Gebreab Kidanu Zewdie, Applying the Fourier, Capon and Maximum Entropy Imaging Techniques to Sao Luis Coherent Radar Interferometer Measurements	23
IRRI-14	Brett Isham, Nonthermal plasma modes in the terrestrial ionosphere.....	23

IRRI-15	Douglas Patrick Drob, Understanding the Response of the Ionosphere to Atmospheric Waves Generated by Tsunamis and Other Geophysical Disturbances	23
----------------	--	----

Long Term Variations of the Ionosphere-Thermosphere

LTVI-01	Jessica Hawkins, Solar Zenith Angle as a Driver of Seasonal Oscillations in the Ionosphere.....	24
LTVI-02	Susan Marcelle Nossal, Thermospheric hydrogen response to increases in greenhouse gases.....	24

Magnetosphere-Ionosphere-Thermosphere Coupling

MITC-01	Brian J. Anderson, Relationships between Birkeland current onset dynamics and IMF/solar wind forcing.....	25
MITC-02	Hassanali Akbari, Aspect-angle dependence study of naturally enhanced ion-acoustic lines.....	25
MITC-03	Taylor Cameron, Electron Energy Dispersion as seen by the ePOP Suprathermal Electron Imager.....	25
MITC-04	Hyunju Connor, Initial results of storm-time IT responses using the OpenGGCM-CTIM global magnetosphere-ionosphere-thermosphere model.....	26
MITC-05	Zan Li, Investigation of EMIC Wave Scattering as the Cause for the BARREL January 17, 2013 Relativistic Electron Precipitation.....	26
MITC-06	Austin Patrick Sousa, A Cubesat Instrumentation Suite for In-Situ Measurements of Wave-Induced Particle Precipitation	27
MITC-07	Barry Mauk, Van Allen Probes Overview and New Resources available via the Mission Gateway.....	27

MidLatitude Thermosphere or Ionosphere

MDIT-01	Timothy Duly, Self-consistent generation of medium-scale traveling ionospheric disturbances (MSTIDs) within the SAMI3 numerical model	27
MDIT-02	Timothy Duly, pyglow: Upper atmosphere climatological models in Python.....	28
MDIT-03	Nathaniel Anthony Frissell, Sources and Characteristics of Medium Scale Traveling Ionospheric Disturbances Observed by a Longitudinally Distributed Chain of SuperDARN Radars Across the United States.....	28
MDIT-04	Yen-Chieh Lin, Model simulation of electron density profile in lower part of ionosphere.....	28

MDIT-05	Levan Lomidze, Magnetic meridional winds in the thermosphere derived from GAIM and their sensitivity to atmospheric model parameters.....	29
MDIT-06	Justin J.E. Mabie, High Altitude Acoustic Wave Generated by Launch of the Cygnus ORB-1 Mission to the ISS.....	29
MDIT-07	Freddy M. Perez Ramirez, MatLab Implementation for Ionosphere Modeling Using B-Spline, VTEC and IRI2012 Models.....	30
MDIT-08	Catherine Sullivan, Magnetically Conjugate Observations of Ionospheric Processes Using All-Sky Imagers in the American Sector	30
MDIT-09	Jie Zhu, Simulating electron and ion temperatures in Global Ionosphere Thermosphere Model	31
MDIT-10	Shih Han Chien, Observations of semidiurnal tidal variability at seasonal and day-to-day time scales from the Boulder Fabry-Perot Interferometer	31
MDIT-11	Rafael Mesquita, A study of the correlation between the midnight temperature maximum signature and the total electron content in the mid-eastern continental United States	31
MDIT-12	Rafael Mesquita, A multi-instrument study of the vertical plasma drift difference associated with the pre-midnight brightness wave signature over the north-eastern Brazilian region.....	32

Polar Aeronomy

POLA-01	William Archer, Ion Thermalization at 500 km	33
POLA-02	Meghan Burleigh, Coupling of Low Altitude Ionospheric Upflow Processes to Ion Outflow	33
POLA-03	Robert Clayton, Localized Ionospheric Cubeswarm Concept	33
POLA-04	Barbara Emery, Sondrestrom Joule Heating Estimates.....	34
POLA-05	Christopher Thomas Fallen, Simulations of the high-latitude ionosphere response to the 25 Feb 2014 X4.9-class solar flare.....	34
POLA-06	Victoriya V. Forsythe, Observations of the high-velocity echoes from the polar E region with new Antarctic SuperDARN radars.....	35
POLA-07	Beatriz Gallardo Lacourt, Ionospheric flow structures associated with auroral beading at the substorm auroral onset	35
POLA-08	Lindsay Victoria Goodwin, Negative AL index excursions and their influence on the high latitude F-region ion temperature at dusk.....	36
POLA-09	Michael Hirsch, Reconstruction of Fine Scale Auroral Dynamics	36
POLA-10	Lucas David Hurd, Joule heating effects of small-scale structure and neutral winds in the high-latitude thermosphere/ionosphere.....	37

POLA-11	Geonhwa Jee, Fabry-Perot Interferometer Installed at Korean Jang Bogo Station (JBS), Antarctica.....	37
POLA-12	Stephen R. Kaeppler, Observations in the E-region ionosphere of kappa distribution functions associated with precipitating auroral electrons and discrete aurorae.....	38
POLA-13	Xianjing Liu, Thermosphere dynamics and composition changes.....	38
POLA-14	Cheng Sheng, Correlation between Poynting flux and soft electron precipitation around the cusp region.....	38
POLA-15	Matthew Ryan Patrick, Time Evolution of Poynting Flux as Observed with the Swarm Satellites.....	38
POLA-16	Gareth W. Perry, Spatiotemporally resolved plasma and electric field structuring associated with a sun-aligned arc over Resolute Bay.....	39
POLA-17	Ja Soon Shim, Systematic assessment of the Ionosphere/Thermosphere models driven by different high latitude drivers.....	40
POLA-18	Tom Slanger, The Compact Echelle Spectrograph for Aeronomic Research (CESAR).....	40
POLA-19	Jeffrey D. Spaleta, Index of Refraction Measurements in the Polar Cap Using the McMurdo Radar.....	41
POLA-20	Boyi Wang, Coordinated observations of polar cap flow channels by all-sky imagers and DMSP.....	41
POLA-21	Ying Zou, Localized polar cap flow enhancement evolution and tracing using airglow patches.....	42
POLA-22	Lucas Liuzzo, High-latitude ionospheric drivers and their effects on wind patterns in the thermosphere.....	42
POLA-23	Lucas Liuzzo, A statistical comparison of coupled thermosphere-ionosphere models.....	43

Solar Terrestrial Interactions in the Upper Atmosphere

SOLA-01	Emine Ceren Kalafatoglu Eyiguler, Quantitative Assessment of the Ionosphere-Thermosphere Model Performances for the Orbit Averaged Storm Time Neutral Density along the CHAMP Satellite Track.....	43
SOLA-02	Jeongheon Kim, A quantitative analysis of solar X class flare effects on ionosonde and GPS TEC data.....	44
SOLA-03	Ying-tsen Lin, Modeling Nitric Oxide in the Lower Thermosphere with measured Solar Soft X-ray Irradiance.....	44

SOLA-04	Ryan M. McGranaghan, Forecasting the Impact of Equinoctial High-Speed Stream Structures on Thermospheric Responses	45
SOLA-05	Jone Peter Reistad, Hemispheric asymmetries in the global aurora and IMF Bx.....	45
SOLA-06	Karthik Venkataramani, Radiative cooling of the Thermosphere by infrared emissions from Nitric Oxide... ..	46
SOLA-07	Justin David Yonker, Amplification of NO Production Rate in the Lower Thermosphere due to Catalysis of O ₂ ⁺	46

CEDAR Workshop – IT Poster Session Abstracts
Day 1 – Tuesday, June 24, 2014

Data Assimilation or Management

DATA-01 A Data Assimilative Comparison of Solar Cycle 24 Magnetic Storms -
by Bust, Gary Steven

Status of First Author: Non-student

Presented by: Kaleb H. Slaatthuag, High School Student

Authors: Gary S. Bust, Kaleb H. SlaatHaug

Abstract: We will use the Ionospheric Data Assimilation Four Dimensional (IDA4D) to compare several magnetic storms from the current solar cycle. We will compare global characteristics of storms such as Dst, IMF Bz, hemispheric power and cross-cap potential with the 3D time evolving response of the ionospheric electron density. We will analyze the storms separately and then cross compare them with each other.

We hope to obtain an improved understanding of both common features and differences across storms, how they relate to coupling between different horizontal regions and across different altitude regimes.

DATA-02 Data fusion from a network of Fabry-Perot interferometers: Estimation of regional thermospheric wind dynamics - by Harding, Brian J

Status of First Author: Student IN poster competition, Masters

Authors: Brian J. Harding, Chenshuo Yue, Jonathan J. Makela

Abstract: The recent development of networks of distributed sensors raises the question of how to optimally interpret the resulting data. Although physics-based data assimilation solves this problem and offers the possibility of predictive modeling, there is often a need to analyze the data free from the assumptions and constraints imposed by a physics-based model. We focus specifically on networks of Fabry-Perot interferometers, which are used to estimate regional thermospheric wind dynamics. Since measurements are sparse and incomplete, the estimation problem is underdetermined. Previous work in this area has assumed that the wind field can be approximated with a polynomial, but this can create artificial structure and smooth over real structure. We show how the estimation problem can be formulated as a regularized inversion, which reconstructs structures only to the extent that they are supported by the data. Posing the problem this way can also provide a quantitative means of optimizing the observing strategy and the locations of future deployments.

DATA-03 Effects of estimating unobserved thermosphere-ionosphere states by data assimilation of FORMOSAT-3/COSMIC data on global ionospheric forecasting - by Hsu, Chih Ting

Status of First Author: Student IN poster competition, PhD

Authors: Chih-Ting Hsu, Tomoko Matsuo, Wenbin Wang, Jann-Yenq Liu

Abstract: The thermospheric temperature, compositions, and wind affect ionospheric electron density distribution through dynamical and chemical ion-neutral coupling mechanisms. This study demonstrates the significance of incorporating ion-neutral coupling into the ionosphere data assimilation to the ionospheric analysis and forecast. Ensemble Kalman filter (EnKF) techniques are used to assimilate synthetic electron density profiles sampled according to the FORMOSAT-3/COSMIC mission into the National Center for Atmospheric Research (NCAR) Thermosphere Ionosphere Electrodynamics General Circulation Model (TIEGCM). The combination of the EnKF and first principles TIEGCM allows a self-consistent treatment of the coupling between the ionosphere and the thermosphere in the forecast and assimilation steps of the Kalman filter. Different combinations of TIEGCM ionospheric state variables and thermospheric variables are considered as part of the EnKF state vector. The unobserved state variables (atomic oxygen ion density, neutral temperature, winds, and composition) are estimated through the assimilation of the observed electron density profiles, thus improving the performance of EnKF analysis and forecast cycle.

DATA-04 Ionospheric Assimilation of Radio Occultation and Ground-based GPS data using Non-stationary Background Model Error Covariance -
by Lin, Chi-Yen

Status of First Author: Student IN poster competition, PhD

Authors: Tomoko Matsuo, Jann-Yenq Liu, Ho-Fang Tsai, Chien-Hung Lin

Abstract: Ionospheric data assimilation is a powerful approach to reconstruct the 3D distribution of the ionospheric electron density from various types of observations. We present a data assimilation model for the ionosphere, based on the Gauss-Markov Kalman filter with the International Reference Ionosphere (IRI) as the background model, to assimilate two different types of total electron content (TEC) observations from ground-based GPS and space-based FORMOSAT-3/COSMIC (F3/C) radio occultation. Covariance models for the background model error and observational error play important roles in data assimilation. The objective of this study is to investigate impacts of stationary (location-independent) and non-stationary (location-dependent) classes of the background model error covariance on the quality of assimilation analyses. Location-dependent correlations are modeled using empirical orthogonal functions computed from an ensemble of the IRI outputs, while location-independent correlations are modeled using a Gaussian function. Observing System Simulation Experiments (OSSEs) suggest that assimilation of TEC data facilitated by the location-dependent background model error covariance yields considerably higher quality assimilation analyses. Results from assimilation of real ground-based GPS and F3/C radio occultation observations over the continental United States are presented as TEC and electron density profiles. This study also presents the OSSEs of data assimilation analyses using FORMOSAT-7/COSMIC-2 (F7/C2) with twelve micro satellites, will be launched in 2016 and 2018. Each micro satellite will be equipped with the appropriate satellite signal receiver to conduct the RO experiment with GNSS and GLONASS. This new mission is expected to yield more than 8,000 RO events per day. By assimilating F7/C2 RO data into our data assimilation model, the global ionosphere specification will be significantly improved. Our new ionospheric data assimilation model that employs the location-dependent background model error covariance outperforms the earlier assimilation model with the location-independent background model error covariance, and can reconstruct the 3D ionospheric electron density distribution satisfactorily from both ground- and space-based GPS observations.

**DATA-05 Specification of the plasmasphere using a new data assimilation approach -
by Nikoukar, Romina**

Status of First Author: Non-student, PhD

Authors: Romina Nikoukar, Gary Bust, and David Murr

Abstract: We present a novel technique for imaging and data assimilation of the topside ionosphere and plasmasphere. The global core plasma (GCP) model is used as an empirical background model for assimilation. The Gauss-Markov Kalman filter technique is used to advance estimates of electron density and background error covariances forward in time.

We incorporate regularization techniques in the assimilation algorithm to stabilize the solution in face of limited data perturbation to prevent non-physical altitudinal variation in density estimates due to limited availability of data. The above-the-horizon observations from the Global Positioning System (GPS) receiver onboard Constellation Observing System for Meteorology, Ionosphere and Climate (COSMIC) satellites are utilized in the assimilation algorithm. The estimation results show reasonable agreement with in-situ density measurements of Defense Meteorological Satellite Program satellites and Van Allen Probes derived densities during geomagnetically quiet and severe storm-time conditions, respectively. The results demonstrate great potential for the use of assimilation of COSMIC above-the-horizon measurements in monitoring and studying the morphology and dynamics of large-scale structures of the electron density in the topside ionosphere and plasmasphere.

**DATA-06 Using Ensemble Simulations to Assess Uncertainty in the Upper Atmosphere
- by Pawlowski, Dave**

Status of First Author: Non-student, PhD

Authors: Aaron J. Ridley, Jeff Flegal

Abstract: One of the difficulties in modeling the Earth's upper atmosphere is in quantifying the myriad of uncertainties within the model itself. Of these, one of the most important sources of uncertainty is in the specification of the external drivers of the upper atmospheric system. In order to better understand the effects uncertain drivers, it is possible to perform simulations of the upper atmosphere using the Global Ionosphere-Thermosphere model (GITM) which capture the range of expected states in the drivers. This approach is taken in this study, in which a statistical analysis of the high-latitude drivers, that aims to quantify the small scale noise, has been utilized to compile ensembles of inputs for use with GITM. Results from these simulations will be presented that indicate that even small variations in the drivers can have a significant impact in the resulting state of the upper atmosphere.

**DATA-07 Assimilative Neutral Wind Bias Correction Scheme for Global Ionospheric
Modeling at Midlatitude - by Sun, Yang-Yi**

Status of First Author: Student IN poster competition, PhD

Authors: Yang-Yi Sun, Tomoko Matsuo, Naomi Maruyama, and Jann-Yenq Liu

Abstract: This study demonstrates the usage of a robust data assimilative procedure, which is applied to correct the model wind biases to enhance the capability of the global physics-based Ionosphere Plasmasphere Electrodynamics (IPE) model. The hmF2 observed by the FORMOSAT-3/COSMIC (F3/C)

radio occultation (RO) technique is utilized to adjust global thermospheric field-aligned neutral winds (i.e., a component of the thermospheric neutral wind parallel to the magnetic field) at midlatitudes according to a linear relationship between time differentials of the field-aligned wind and hmF2. The adjusted winds are further applied to drive the IPE model, which is built upon the Field Line Interhemispheric Plasma (FLIP) model with a realistic geomagnetic field model and empirical model drivers. The comparison of the modeled electron density with the observations of F3/C and ground-based GPS receivers at the 2012 March Equinox suggests that the modeled electron density can be significantly improved, especially in the midlatitudes of the Southern Hemisphere. Moreover, the F3/C observation, the IPE model, and the wind bias correction scheme are applied to study the 2012 Southern Hemisphere Midlatitude Summer Nighttime Anomaly (southern MSNA)/Weddell Sea Anomaly (WSA) event at the December Solstice for examining the role of the neutral winds in controlling southern MSNA/WSA behavior over different longitudes. With the help of the wind bias correction scheme, the IPE model comprehensively reproduced the F3/C observed southern MSNA/WSA features. The apparent eastward movement of the southern MSNA/WSA features in the local time coordinate is primarily caused by the longitudinal variation in declination angle of the geomagnetic field that controls the field-aligned projection of both geographic meridional and zonal neutral winds.

Equatorial Thermosphere or Ionosphere

EQIT-01 LISN network: TEC observations over South America - by Espinoza, Juan C

Status of First Author: Student NOT in poster competition, Undergraduate

Authors: Juan C. Espinoza, Cesar Valladares

Abstract: The Low-Latitude Ionospheric Sensor Network (LISN) have been recording GPS data since late 2007, the LISN data, as well as, data from GPS receivers belonging to other instrumental networks has been used to map Total Electron Content (TEC) over the South American continent. In this poster we present the regional day-to-day variability of the TEC measurements during a low solar activity period (2009-2010) and during the ascending solar activity phase (2011-2012).

Besides the regional TEC maps we also present an overview of the LISN database. Users can derive different data products from measurements conducted by GPS receivers, ionosondes and magnetometers.

EQIT-02 The equatorial ionosphere's response to the October 2012 geomagnetic storms - by Hairston, Marc

Status of First Author: Non-student

Authors: Marc R Hairston, W Robin Coley, R A Heelis

Abstract: The CINDI thermal plasma instruments on the C/NOFS spacecraft measure the ion density, temperature, composition, and flow in the equatorial ionosphere between ~395 and ~750 km. During October 2012 there were three large geomagnetic storms within two weeks (1 October, 8 October, and 13 October). We have examined the CINDI observations of these parameters before, during, and after the storm events to determine the equatorial ionosphere's response to these storms. In general the clearest signature in all three storms is the temperature which rises and then returns to normal over the course of a day after the storm onset. However this response is only seen below a certain altitude (which varies for each storm), thus we conclude the ion heating comes from contact with the neutral particles in the thermosphere and their response to the storm.

EQIT-03 Equatorial Electrojet Irregularities- New Fluid Approach and Simulation -
by Hassan, Ehab

Status of First Author: Student IN poster competition, PhD

Authors: Ehab Hassan, Wendell Horton

Abstract: A new approach for the coupling between Farley-Buneman (type-I) and Gradient-Drift (type-II) instabilities in the Equatorial Electrojet using a fluid model. The simulation results reproduce some of the Incoherent-backscatter Radars and in-situ Rocket data such as (1) the ion-acoustic drift speed of the irregularities in the saturated state, and (2) the generation of a meter-scale irregularities that dominate the echoes spectrum.

EQIT-04 Boston University All-Sky Imager at the Jicamarca Radio Observatory -
by Hickey, Dustin A.

Status of First Author: Student IN poster competition, PhD

Authors: Carlos Martinis, Catherine Sullivan, Joei Wroten, Jeff Baumgardner, Michael Mendillo, Marco Milla, Luis Navarro, and Dave Hysell

Abstract: In March 2014 an all-sky imager was installed at the Jicamarca Radio Observatory. The imager contains four filters to observe processes in the mesosphere (5577 Å and 6950 Å) and in the thermosphere, near the F-region peak (6300 Å and 7774 Å). In this work optical data are compared with Jicamarca radar data. ASI data has been analyzed to identify brightness waves, mesospheric gravity waves, airglow depletions associated to equatorial spread F (ESF), and medium scale travelling ionospheric disturbances (MSTIDs). We present cases of ESF occurrence, observed as dark north-south oriented structures in 6300 Å. The Jicamarca incoherent scatter radar (ISR) provides ion temperature, electron temperature, plasma drifts, and electron density. These ionospheric parameters are used as inputs in a model that provides height, volume emission rate and total emission from the airglow at 6300 Å and 7774 Å. When run in the Jicamarca Unattended Long-term Investigations of the Ionosphere and Atmosphere (JULIA) mode, the in-situ optical structures associated with ESF can be compared with the radar data. In addition, ASI data have been analyzed to detect brightness waves, an increase in brightness in 6300 Å airglow associated with the midnight temperature maximum (MTM). The installation of the BU ASI at Jicamarca provides a clear 2-dimensional view of spatial and temporal evolution of the ionosphere and processes occurring there. This view will be enhanced when other existing instruments at the observatory are incorporated in the analysis.

EQIT-05 Equinoctial asymmetry of transition heights in topside ionospheric profiles -
by Hong, Junseok

Status of First Author: Student IN poster competition, Undergraduate

Authors: Junseok Hong, Eunsol Kim, Jeong-Heon Kim, Yong Ha Kim

Abstract: In order to investigate ionospheric irregularities at low latitudes, we analyzed topside ionospheric sounder data from Alouette-1. Among the data of topside electron density profiles covering the period of 1962 - 1972, we chose topside profiles measured near 290° longitude during night time (17-05LT) at low latitudes (20°S - 20°N) where plasma bubbles, as typical ionospheric irregularities, are known

to occur frequently. We find that profiles of 60 days show 10% or more difference between neighboring profiles, indicative of ionospheric irregularities. We derive transition heights from O⁺ to H⁺ at which an electron density is twice an O⁺ density. The transition heights are generally higher near the magnetic equator (~10°S at 290° longitude) than at northern latitudes, implying that the protonosphere is confined higher altitudes near the magnetic equator. During summer, when the subsolar point is located in the northern hemisphere, the difference of transition heights between northern and southern hemispheres is small, whereas it is large during winter. However, the difference of transition heights is smaller in spring equinox than in fall equinox, implying other influence than that from the sun. This may be related to the phenomenon known as equinoctial asymmetry, which was noted in different occurrences of equatorial ionospheric irregularities in spring and fall equinox months. It has been proposed that meridional winds in the thermosphere may cause this asymmetry. We will present results of the SAMI2 model that test whether meridional winds can explain the equinoctial asymmetry of transition heights in the topside ionospheric profiles.

EQIT-06 Westward neutral winds in the postsunset equatorial Thermosphere -
by Kiene, Andrew Devon

Status of First Author: Student IN poster competition, PhD

Authors: A. Kiene and M. F. Larsen

Abstract: The Guara sounding rocket campaign involved, in part, four sounding rockets that released chemical tracers at different altitudes and latitudes on two consecutive nights in September 1994. Two rockets were launched each night, providing E-region chemical tracer neutral winds at the equator and ~450 km further north, as well as an F-region Barium/Strontium cloud at the equator. The E-region winds were derived at the time, but the Ba/Sr winds were never published due to difficult triangulation conditions. Revisiting the Ba/Sr data has produced a unique dataset showing simultaneous measurements of equatorial neutral winds in the E and F regions, as well as F-region plasma drifts from the ionized Barium. Generally, it is expected that F-region neutral winds begin to reorient eastward as the sun sets, driving an enhancement of the eastward electric field that in turn enhances vertical E x B drifts associated with the onset of equatorial spread-F. However, on both nights, the Ba/Sr observations show strongly westward neutral winds in the F-region, as well as significant vertical shear in the region between 250 and 280 km.

EQIT-07 Altitude Structure of the Equatorial Thermosphere Anomaly -
by Hsu, Vicki

Status of First Author: Student IN poster competition, PhD

Authors: Vicki W. Hsu and Jeffrey P. Thayer

Abstract: The equatorial thermosphere anomaly (ETA) is a feature of the upper atmosphere that is characterized by two crests at ±20-30° and a trough at the magnetic equator in neutral mass density and temperature. Recently, the formation mechanism of the ETA has been significantly developed, and its variations with local time, solar flux, and nonmigrating tides have been evaluated. In this study, we analyze the altitudinal variations of the ETA using observations from the Challenging Minisatellite Payload (CHAMP) and Gravity Recovery and Climate Experiment (GRACE) satellites, and the National Center for Atmospheric Research Thermosphere Ionosphere Electrodynamics Global Circulation Model (NCAR-TIEGCM). We attempt to identify the ETA signature in the CHAMP and GRACE neutral mass density observations, and compare them to TIEGCM simulations. The model is also used to explain what processes or terms contribute significantly to the altitude structure of the ETA.

EQIT-08 Zonal drifts from all-sky imaging observations and CINDI data: magnetically conjugate behavior and latitudinal shear - by MacInnis, Rebecca

Status of First Author: Student IN poster competition, Undergraduate

Authors: R.Macinnis, C.Martinis, C. Sullivan, J. Baumgardner, R. Heelis, M.Hairston

Abstract: Images from ground base all sky imagers at Arecibo, Puerto Rico (18.3°N, 66.8°W, 28° mag lat), Mercedes, Argentina (34.7°S, 59.4°W, 25° mag lat), and El Leoncito, Argentina (31.8°S, 69.3°W, 18° mag lat) are analyzed to investigate ionospheric processes in the American sector at low and middle latitudes. Optical data are complemented by data collected by the Couple Ion Neutral Dynamics Investigation (CINDI) instrument aboard the Communication/Navigation Outage Forecasting System (C/NOFS) satellite. Ionospheric structures associated with equatorial spread F have been observed to occur at both hemispheres along common magnetic flux tubes, i.e., they present magnetic conjugacy. Zonal plasma drifts are computed from the motion of airglow depletions associated with equatorial Spread-F (ESF). Results from Mercedes and Arecibo ASIs are compared to understand if there is any influence of the South Atlantic Magnetic anomaly (SAMA), a region in the southern hemisphere where the intensity of Earth's magnetic field decreases by ~ 30%. This study used optical data from 2011 to 2013. Several common nights were used to obtain zonal speeds at the conjugate sites. Drifts are also computed at different latitudes and compared with C/NOFS measurements mapped along field lines to the FOV of the ASI. Geomagnetic storm effects are investigated in a case study, 25 October 2011. Detailed analysis shows that depletions in the northern hemisphere are thinner and that they reach higher latitudes when compared with the structures in the Southern hemisphere.

EQIT-09 The Tropical Ionization Anomaly - by Valladares, Cesar Enrique

Status of First Author: Non-student

Authors: Vince Eccles

Abstract: Continuous and regional measurements of total electron content (TEC) over the Americas have revealed that quite frequently the largest TEC values reside over Central America. These unexpected and anomalous TEC values have not been reported before. They are observed during the June solstice afternoon hours, last for a few hours, are constrained to regions of eastward magnetic declination and occur at magnetic latitudes poleward of 20°. During the December solstice, similar TEC enhancements are seen over the southern coast of Brazil, also poleward of 20°, but in a region where the declination is westward. It is proposed and demonstrated using a physics-based model of the low-latitude ionosphere, that the TEC enhancements are produced by the neutral winds blowing at longitudes where the Earth's magnetic declination is different from zero. Due to their anomalous character, the TEC enhancements have been designated as the tropical ionization anomaly.

**EQIT-10 Equatorial Electric Fields in the Brazilian and Peruvian Sectors -
by Moro, Juliano**

Status of First Author: Student NOT in poster competition, Masters

Authors: C. M. Denardini, L. C. A. Resende, S. S. Chen, N. J. Schuch

Abstract: There have been several important breakthroughs studies in the last few years about the equatorial electric fields in several longitudinal sectors. These studies have shown that E-region dynamo electric field plays an important role in several ionospheric phenomena. In this work, we present the results of the electric fields estimated from the backscattered echoes obtained by the 50 MHz coherent scatter radar (also known by RESCO) observed over São Luís, Brazil, (2.3°S, 44.2°W) and by the Jicamarca Unattended Long-term Studies of the Ionosphere and Atmosphere (JULIA) coherent scatter radar, observed over Jicamarca, Peru, (11.95°S, 76.87° W). The results are discussed in terms of some coincident quiet time data ($Kp < 3$) acquired by RESCO and JULIA in the last solar minimum (2001-2009).

EQIT-11 Observations of low-latitude irregularities during low and moderate solar activity - by Pacheco, Edgardo

Status of First Author: Non-student, PhD

Authors: E.E. Pacheco, E. Yizengaw, M. Milla, C.E. Valladares, K. Groves, R.A. Heelis, R. Stoneback, P. Roddy

Abstract: We use ground-based and satellite measurements to study the features of ionospheric irregularities at low latitudes during the last solar minimum and the ascending phase of solar cycle 24. In this study, we present the longitudinal variability of plasma depletions and scintillation activity as a function of local time, seasons and solar activity. Spatial and temporal distributions of total electron content depletions (TEC) are obtained from the LISN, SCINDA and IGS ground-based GPS networks to examine the occurrence probability and characteristics of plasma depletions and their correlation with scintillation activity at different longitudes. In addition, we use measurements from the C/NOFS satellite to study the longitudinal distribution of the background density during the occurrence of the irregularities and the density perturbations. Furthermore, measurements from the Jicamarca radar provide a more detailed description of the occurrence and evolution of the irregularities as a function of altitude in the western South American sector.

EQIT-12 MELISSA: A new coherent backscatter radar interferometer for the Brazilian sector - by Rodrigues, Fabiano

Status of First Author: Non-student, PhD

Authors: Fabiano S Rodrigues and Gebreab Zewdie (The University of Texas at Dallas, Richardson, TX, USA) Marco Milla, Marcos Inonan, Rommel Yaya, and Alejandro Belleza (Jicamarca Radio Observatory, Lima, Peru) Eurico R. Paula, Acacio C. Neto, and Luis Sergio F. Gomes (Instituto Nacional de Pesquisas Espaciais, Sao Jose dos Campos, SP, Brazil)

Abstract: We report successful first observations made by a new 30 MHz coherent backscatter radar interferometer deployed in the Brazilian sector. The MELISSA (Measurements of Equatorial and Low-latitude irregularities over Sao Luis, South America) radar replaces the system that operated in the magnetic equatorial site of Sao Luis between 2000 and 2012. The new system was developed and deployed through an international scientific collaboration between the University of Texas at Dallas, the Jicamarca Radio Observatory (JRO), and the Brazilian National Institute for Space Research (INPE).

The digital receiver and acquisition system were designed and developed at Jicamarca. The Jicamarca Acquisition System Radar (JASR) is a multi-channel system based on software-defined radio architecture. A new web interface facilitates the configuration of experiments. For transmission, we used a solid-state transmitter built by ATRAD. The dual-output, 10% duty cycle transmitter operates at 29.795 MHz, and delivers 16 kW peak power. We also used the set of 4 antennas (4x4 Yagis) from the old radar system for

the new observations. The antennas are spaced in such a way that correlations for 6 different baselines along the magnetic zonal direction can be computed.

The main objective of the system is to make semi-routine observations of F-region field-aligned irregularities, but it can also make measurements of electrojet, and 150-km echoes irregularities under the right conditions. The deployment and first measurements were made in March 2014. Since then, semi-routine measurements of nighttime F-region irregularities are being made. Examples and analysis of the first measurements will be presented.

EQIT-13 On the magnitude of equatorial pre-reversal enhancement of the ionospheric zonal electric field and equatorial topside irregularities -
by Smith, Jessica Mae

Status of First Author: Student IN poster competition, Masters

Authors: J. M. Smith and F. S. Rodrigues (The University of Texas at Dallas, Richardson, TX)
M. Milla (Jicamarca Radio Observatory, Lima, Peru)

Abstract: The pre-reversal enhancement (PRE) of the zonal equatorial electric field that is observed around sunset hours is believed to be the most important factor dictating the occurrence of equatorial spread F (ESF) irregularities (Fejer et al. (1999), Basu et al. (1996), Abdu et al. (1983)). Topside echoes observed by ground-based coherent radars are commonly associated with dramatic ionospheric disturbances caused by fully developed ESF events (plasma bubbles or depletions).

The Jicamarca radar in Peru is capable of making measurements of echoes caused by thermal plasma fluctuations (incoherent echoes) as well as echoes caused by non-thermal fluctuations (coherent echoes). The incoherent echoes are used to derive background plasma parameters, including vertical and zonal components of the ionospheric plasma motion. Coherent echoes, on the other hand, can be used to infer the occurrence and morphology of field-aligned irregularities, including those associated with ESF.

We take advantage of the Jicamarca capability to carry out a comprehensive investigation of the relationship between the evening vertical plasma drifts and the occurrence of pre-midnight topside F-region irregularities. Measurements made between 1994 and 2013 are particularly important thanks to advances in the drift measurements made by Kudeki et al. (1999).

We used the Jicamarca measurements to determine mean vertical plasma drifts in the evening sector and the occurrence of topside irregularities. We investigated the magnitude of the drifts between 17:00 LT and 20:00 LT and the detection of coherent echoes between 19:00 LT and local midnight. We are particularly interested in the occurrence of topside irregularities without a significant PRE.

Analyses of 114 geomagnetically quiet nights of observations, led us to find interesting cases of pre-midnight topside irregularities when no significant PRE was detected. The echoes, however, do not follow the typical pattern caused by topside ESF bubbles (radar plumes). Our results show that a PRE of significant magnitude in the mean drifts, as observed at a given location, is not a necessary condition for the observation of topside irregularities over that location. The results also signal the possibility of other instability mechanisms leading to equatorial topside irregularities.

EQIT-14 First steps towards the implementation of a cognitive radar to study plasma instabilities near the Peruvian Andes - by Sorbello, Robert Michael

Status of First Author: Student NOT in poster competition, PhD

Authors: Karim Kuyeng, Julio Urbina

Abstract: A cognitive radar system is composed of three key components: 1) intelligent signal processing, which builds on radar interactions from the surrounding environment, 2) receiver feedback which is utilized by the transmitter to facilitate an intelligent response to detected signals, and 3) preservation of radar echo information contents. We describe the implementation of a VHF coherent imaging radar in Huancayo, near the Peruvian Andes to initiate continuous monitoring of the plasma structuring in the equatorial ionosphere. The new radar system will utilize cognitive sensing techniques and complement the ionospheric observations conducted by the Jicamarca incoherent scatter radar (ISR), located about 170 km to the west of Huancayo along the geomagnetic equator. The main purpose of the new system will be to obtain uninterrupted images of ionospheric structuring and drifts from Huancayo, which are only probed and sampled intermittently from Jicamarca due to the operation costs and scheduling issues of the more powerful incoherent scatter system. The proposed system will work in two stages: 1.) Classifying the occurrences observed in the atmosphere, and 2.) transmitting an optimal waveform to illuminate and process areas of interest. In this paper, we present classification techniques to correctly identify the following geophysical equatorial echoes: Spread-F, electrojet, 150 km echoes, and meteors. These events are each categorized by signal parameters with known distributions, e.g., signal-to-noise ratio, changes in range, instantaneous frequency, periodicity, etc. We will provide an overview of the classification algorithm used to distinguish returns from the various equatorial phenomena. A Gaussian Mixture Model (GMM) has already been implemented to classify meteor events at mid latitudes. The same algorithm has been extended to include the Spread F, 150 km echoes, and electrojet. Previously, classifying the meteor events involved capturing whole process because of the feature selection of the GMM. With the addition of these events however, new procedures are used because the duration of the phenomenon sustains for multiple hours. Therefore, classification must be made with a small fraction of the entire event. The purpose of this approach is to formalize the first step towards the cognitive radar, which can then be further extended to adjusting the waveform parameters for optimal responses. In addition to the classification algorithm, results of a short campaign conducted at Jicamarca will be discussed. Implications of the results for the future system in Huancayo will be determined.

EQIT-15 Signal Chain Software for Jicamarca Radar - by Suarez Munoz, Daniel

Status of First Author: Student NOT in poster competition, Undergraduate

Authors: Miguel Urco, Alexander Valdez, Marco Milla

Abstract: The Signal Chain Project at Jicamarca has the goal of developing software libraries for radar signal processing. These libraries are based on the Python programming language and are organized in three classes: Voltage, Spectrum and Correlation. Each class has operations like incoherent and coherent integrations, profiles selector, channels selector, coherence calculation, noise estimation, FFT, correlations, IOs and plotting libraries. These libraries can be setup according to the radar experiment requirements in simple steps which are described in this poster. Signal Chain has a friendly user interface with predefined operations for use by regular users; more advanced users can set up experiments using a python script.

Instruments or Techniques for Ionospheric or Thermospheric Observation

ITIT-01 Measurement of Neutral Winds and Gradients in the Lower Thermosphere with Multi-Point, Chemical-Release Sounding Rocket Payloads - by Andersen, Carl

Status of First Author: Student IN poster competition, PhD

Authors: Carl Andersen, Mark Conde

Abstract: Sounding rocket payloads capable of deploying multi-point chemical releases provide a unique tool for investigating the properties of the lower thermosphere. This type of payload consists of a collection of sub-payloads that are propelled laterally out of the rocket during flight. Each contains a canister of liquid tracer (such as tri-methyl aluminum) which, after separating from the main rocket, is dispersed by explosive detonation. The result is a luminous "puff" that can be tracked by triangulation using images taken from several ground stations, producing wind vector velocities with typical uncertainties of just 1-2 m/s. A deployment of puffs throughout a 3-dimensional volume spanning approximately 100x100 km horizontally and from 100 to 180 km altitude, vertically, makes it possible to measure the height profiles of all nine first-order spatial gradients of the neutral wind vector in the lower thermosphere.

ITIT-02 First ever cross-comparison of thermospheric neutral wind measured by narrow and wide field optical Doppler spectroscopy -
by Dhady, Manbharat Singh

Status of First Author: Student IN poster competition, PhD

Authors: J. W. Meriwether, M. Conde, D. Hampton

Abstract: Optical remote sensing is a very powerful tool for studying thermospheric neutral dynamics, and many variants of it have been developed. Because the techniques are somewhat indirect, it is important for the various methods to be cross validated. Scanning Doppler imagers (SDI) and Fabry-perot Interferometers (FPI) has been used in mapping thermospheric neutral winds for decades. Both are based on Doppler spectroscopy of naturally occurring optical emissions from the thermosphere, and both use Fabry-Perot etalons to obtain the required spectral resolution. They are entirely different in technical perspective, modes of operation, data collection, and data analysis. Ishii et al. [2001] compared vertical wind inferred by these two techniques, but horizontal neutral wind inferred by SDI has never been cross compared before. Fortunately in Alaska, SDI and FPI are monitoring common volumes of the thermosphere at the same wavelength (630nm). In the present study, we present the first ever detailed cross-comparison of F-region horizontal neutral winds inferred by SDI and FPI. Horizontal neutral winds inferred by monostatic SDI, bistatic SDI, and bistatic FPI (with and without vertical wind) were cross compared for total 7 nights from 2010, collecting data from four observatories (two SDI and two FPI) in Alaska. The results of this study show a high degree of correlation between SDI and FPI measured diurnal behavior of line-of-sight (LOS) wind. The variability recorded in FPI LOS wind was stronger than SDI. Every night there were many instances when temporal characteristics of the high frequency fluctuations in time series recorded by SDI and FPI were very similar, which suggests that those fluctuation recorded by both instruments are geophysical. SDI produces high resolution maps of thermospheric neutral wind over a wide geographic region of thermosphere. Angular size of the smallest zone of SDI is much larger than for FPI. The suppression in fluctuations in SDI LOS wind compared to FPI suggests the presence of local scale structures with size smaller than roughly 40 km. Zonal and meridional wind estimated by monostatic SDI, bistatic SDI, and bistatic FPI wind fits were in close agreement. Mapped wind fields showed that most of the discrepancies between estimated winds by two instruments occurred when neutral wind speed was slow. High neutral wind speed presumably suppressed structures in neutral wind field.

ITIT-03 Possible measurements of low-altitude ion conics from the MICA sounding rocket - by Fernandes, Philip

Status of First Author: Student IN poster competition, PhD

Authors: Fernandes, P.A. and Lynch, K.A.

Abstract: The MICA sounding rocket launched on 19 Feb. 2012 into several discrete, localized arcs in the wake of a westward traveling surge. In situ and ground-based observations provide a measured response of the ionosphere to preflight and localized auroral drivers. Initial analysis of the in situ thermal ion data indicate possible measurement of an ion conic at low altitude (< 325 km). In the low-energy regime, the response of the instrument varies from the ideal because the measured thermal ion population is sensitive to the presence of the instrument. The plasma is accelerated in the frame of the instrument due to flows, ram, and acceleration through the sheath which forms around the spacecraft. The energies associated with these processes are large compared to the thermal energy. Correct interpretation of thermal plasma measurements requires accounting for all of these plasma processes and the non-ideal response of the instrument in the low-energy regime. This is an experimental and modeling project which involves thorough analysis of ionospheric thermal ion data from the MICA campaign. Analysis will include modeling and measuring the instrument response in the low-energy regime as well as accounting for the complex sheath formed around the instrument. The final step will be the development of a forward model, in which plasma parameters of the thermal plasma are propagated through the sheath and instrument models, resulting in an output which matches the in situ measurement. In the case of MICA, we are working toward answering the question of the initiating source processes that result, at higher altitudes, in well-developed conics and outflow on auroral field lines.

ITIT-04 First Balmer-a Airglow Temperature Observations using Field-Widened Spatial Heterodyne Spectroscopy - by Gardner, Derek

Status of First Author: Student NOT in poster competition, PhD

Authors: D. D. Gardner, E. J. Mierkiewicz, F. L. Roesler, J. M. Harlander, K. P. Jaehnig, L. M. Haffner, S. M. Nossal, J. W. Percival

Abstract: We present first-light observations of the Balmer-alpha airglow line (6562.7A) from Pine Bluff Observatory (PBO), WI, using a field-widened Spatial Heterodyne Spectrometer (FW-SHS). FW-SHS is a relatively new Fourier-transform instrumental technique that combines large throughput advantage with high spectral resolution and a long spectral baseline in a compact instrument with no moving parts. These characteristics make the FW-SHS well suited to spectroscopic studies of faint, diffuse-source emission lines, and in particular, the possibility to constrain exospheric Hydrogen population dynamics from observed Balmer-a line profiles at high shadow altitudes. An absolute intensity cross-calibration method for FW-SHS using galactic sources will be shown, and empirical performance characteristics and results compared to the PBO Fabry-Perot Interferometer observations previously obtained.

ITIT-05 Ionospheric Inversion Using OII 83.4 nm Observations - by Geddes, George R.

Status of First Author: Student NOT in poster competition, PhD

Authors: George Geddes, Ewan Douglas, Supriya Chakrabarti, Tim Cook, Andrew Stephan

Abstract: Observations of OII 83.4 nm dayglow emission profiles can be used to constrain ionospheric parameters due to the resonant scattering of this line. Ionospheric parameters obtained by inverting extreme ultraviolet emission profiles from the Remote Atmospheric and Ionospheric Detection System (RAIDS) are compared with ionosonde driven predictions in order to investigate how best to improve constraints on this inverse problem. Direct measurement of the photoionization source via the OII 61.7 nm line is considered as a method for improving constraints on these parameters.

ITIT-06 Versatile four channel tunable hyperspectral imager for remote sensing -
by Goenka, Chhavi

Status of First Author: Student IN poster competition, PhD

Authors: C. Goenka, J. L. Semeter, J. Noto, H. Dahlgren, R. Marshall, J. Baumgardner, J. Riccobono, M. Migliozzi, D. Hampton, M. Hirsch

Abstract: Hyperspectral imagers provide spatial and spectral information, finding use in various remote sensing applications such as terrestrial vegetation analysis, analysis of aeronomical signals, astronomy, identification of minerals, medical imaging, etc. A wavelength tunable hyperspectral imaging system, which captures data in multiple wavelengths simultaneously, is capable of providing such spatio-spectral data cubes at high temporal resolution, making it truly versatile. Such a system has been designed and tested for three applications, viz. auroral imaging, outlier detection and terrestrial landscape analysis. Preliminary measurements and analyses from these tests will be presented. The challenges posed by each of these applications for the design and performance of the system will also be discussed.

ITIT-07 Optical Characterization Methods for Assessing Threat of Spacecraft
Electrical Anomaly due to Hypervelocity Impact Plasma -
by Hew, Monica

Status of First Author: Student IN poster competition, Masters

Authors: Monica Y. Hew, Sigrid Close, and Ivan Linscott

Abstract: Meteoroids and orbital debris, collectively referred to as hypervelocity impactors, travel between 7 and 70 km/s in free space. When they impact spacecraft the energy conversion from kinetic to ionization/vaporization occurs within a very brief timescale and results in a small and dense expanding plasma. This plasma can produce radio frequency (RF) emission that could potentially lead to electrical anomalies within the spacecraft. Additionally, space weather, such as solar activity and background plasma, can set up spacecraft conditions that can amplify the damages done by these impacts. In previous projects, numerical plasma model and experimental hypervelocity impact tests have been done to study the plasma properties, such as temperature and compositions. In this research, an optical detection method is proposed, which consists of two parts. The first part is a non-resonant laser absorption test, which backlights the plasma with a laser and records its absorbance. The temperature and density profile can be inferred from the measured absorption coefficients. The second part uses a quantitative Schlieren imaging technique to film the expanding plasma, and the density gradient profile can be extracted. With a known density boundary condition, the density of the expanding plasma can be resolved. This method will directly provide a spatially resolved 2D density and temperature profiles, instead of the time resolved discrete density measurements at designated locations as in previous projects. Additionally, the optical method is less intrusive when compared to the electric field sensors, which might distort the electromagnetic fields around the plasma, used in previous experiments.

ITIT-08 Preliminary results of the PSU All-sky Radar Interferometry System
(PARIS) - by Kuyeng Ruiz, Karim M.

Status of First Author: Student NOT in poster competition, Masters

Authors: Alex Hackett, Ryan Seal, Julio Urbina

Abstract: After the first radar prototype, a change of operation frequency had to be done from 50MHz to 40MHz. This poster shows the different modifications of the system plus the results obtained.

**ITIT-09 Newly Revised Helium Resonance Fluorescence LiDAR -
by Mangogna, Tony**

Status of First Author: Student IN poster competition, PhD

Authors: Tony Mangogna, Gary Swenson

Abstract: The helium resonance fluorescence LiDAR transmitter has been redesigned for transport to a remote facility. This new transmitter will be used with a large aperture receiver in order to attempt the first resonantly scattered photon detection from helium using LiDAR.

**ITIT-10 Design for Miniaturized Time-of-Flight Reflectron Mass Spectrometer for
Upper Atmosphere Density Measurements -
by Pyle, Michelle Lynn**

Status of First Author: Student IN poster competition, Masters

Authors: Ryan L. Davidson; Michelle L. Pyle; Charles M. Swenson;

Abstract: Variations of gas density and composition in Earth's upper atmosphere create trajectory and orbit control problems for satellites of all sizes. Satellite orbits must be manually adjusted to compensate for changes in the upper atmosphere environment, and complex modeling techniques are used to help predict how extraterrestrial events may cause these variations. Mass Spectrometers are among an array of instruments used to explore earth's upper atmosphere and other space environments. Normally, these instruments are substantial in size and deployed on larger satellites and space probes. Launching these larger instruments for studying the variations in Earth's upper atmosphere is not practical due to the cost of putting larger satellites into orbit. The proposed miniaturized time-of-flight mass spectrometer will have a mass resolution and range of measurement capable of measuring the free ion density of Earth's Thermosphere while operating within the power and space constraints of a Cube satellite to avoid the prohibitive cost to launch. Elements from existing time-of-flight mass spectrometer designs, including the use of an ion mirror and signal processing techniques, will be used along with a new concept for the ion flight path to achieve the desired range and resolution.

**ITIT-11 Estimation of Self-Clutter for HF Ionospheric Radars that Employ the
Multi-pulse Technique - by Reimer, Ashton Seth**

Status of First Author: Student IN poster competition, PhD

Authors: Ashton S. Reimer, Glenn C. Hussey

Abstract: Some ionospheric radars, such as the Super Dual Auroral Radar Network (SuperDARN) radars, take advantage of long-distance multi-hop propagation that is possible in the high-frequency (HF) band. The multi-pulse technique is used to overcome range-doppler ambiguities characteristic of overspread ionospheric targets (long range: > 1000 km and high velocity: ~1 km/s) at the expense of introducing self-

clutter. Farley (1972) first discussed estimating this self-clutter for incoherent scatter radars assuming uniform scattering. The present study discusses a generalized algorithm for more accurately estimating self-clutter by utilizing measurements of echo power, allowing for an improved estimate of the mean square error in the radar observations.

Farley D. T. (1972). Multiple-pulse incoherent-scatter correlation function measurements. *Radio Science*, Vol 7. Num 6. pg. 661-666.

ITIT-12 Determination of an Optimal Pulse-Repetition Time for SuperDARN radars
- by Reimer, Ashton Seth

Status of First Author: Student NOT in poster competition, PhD

Authors: Ashton S. Reimer, Glenn C. Hussey

Abstract: The Super Dual Aurora Radar Network (SuperDARN) radars are used to measure the magnetospheric plasma circulation via F-region irregularities. Often these irregularities are overspread, therefore SuperDARN radars employ a multi-pulse technique to overcome these range-doppler ambiguities. The multi-pulse technique may be characterized by three parameters: number of pulses, pulse width, and pulse repetition time. A case study is presented for SuperDARN radars wherein the optimal choice of pulse repetition time is discussed. The method presented is valid for all radars utilizing the multi-pulse technique.

ITIT-13 High speed multi-antenna radar receiver - by Sun, Weiwei

Status of First Author: Student NOT in poster competition, PhD

Authors: Weiwei Sun, John D. Sahr

Abstract: We present a new receiver as the fourth generation of the Manastash Ridge Radar (MRR), which is a distributed passive radar system used for ionospheric physics and engineering development. Our motivation in designing this system was two-fold: we desired access to more downconverted bandwidth, and we also wished collect VHF and UHF signals on the same antenna. The new system directly samples four antennas at up to 5 billion samples per second. The system is comprised of Reconfigurable Open Architecture Computing Hardware (ROACH), which was developed by the CASPER radio astronomy collaboration. This system permits unaliased Nyquist sampling well into the UHF spectrum, while providing simultaneous access to VHF and UHF illuminators without duplication of the RF signal path. Among other things, the entire FM broadcast band is now accessible simultaneously. DTV signals can not only be used for aircraft detection, but also can be used for geophysics applications, such as E region field-aligned irregularities. With the first and second generation of MRR receivers, we provided observations of ionospheric turbulence at FM frequencies (around 100 MHz). The new receiver will permit simultaneous VHF and UHF observation of E-region irregularities with a single set of antennas. UHF interferometry will have five times finer resolution than the VHF using the same baselines.

ITIT-14 Plasma Motion Induced Artifacts in 3-D Incoherent Scatter Radar -
by Swoboda, John P

Status of First Author: Student IN poster competition, PhD

Authors: John Swoboda, Joshua Semeter

Abstract: By leveraging electronically steerable phased array antenna technology, incoherent scatter radars have now become full three-dimensional remote sensors for ionosphere plasmas. Currently these systems are operating in the high latitude region where the ionosphere is highly dynamic in both space and time. These systems are giving researchers an unprecedented look at the ionosphere that they have not had in the past.

Because of the highly dynamic nature of the ionosphere in this region it is important to differentiate between artifacts and the true behavior of the plasma. Often the three dimensional data is fitted in polar coordinates and then the parameters are interpolated to a Cartesian grid. This and other sources of error could be effecting reconstructions of the plasma parameters

In this study we explore the impacts of fast moving plasma progressing through the field of view of the radar on the reconstruction of the three dimensional parameters. We pose the problem as a linear inverse problem for the lags of the plasma autocorrelation function. We will show the impact of the plasma through simulation from a full 3-d incoherent scatter radar model. From there we can apply methods from image and video processing to attempt to correct for the artifacts.

ITIT-15 The Optical Profiling of the Atmospheric Limb (OPAL) CubeSat Experiment - by Tatton, Nicole

Status of First Author: Student NOT in poster competition, Undergraduate

Authors: Chad Fish, Jaden Miller, Nikki Tatton, Alan Marchant, Mike Taylor, Charles M Swenson, Ludger Scherliess, Andrew Christensen, Dennis McCarthy, Matt Jeppsen

Abstract: The Optical Profiling of the Atmospheric Limb (OPAL) is a recently selected mission in the NSF CubeSat-based Science Missions for Geospace and Atmospheric Research program. The objective of the proposed mission is to understand the thermospheric temperature signatures of the dynamic solar, geomagnetic and internal atmospheric forcing. A student team, supported by professional scientists and engineers will design, build and execute the OPAL Instrument and mission. OPAL will measure lower thermospheric temperatures from 90–140 km altitude by observing the daytime O₂ A-band (near 762nm) emission with a high-sensitivity, hyper-spectral limb imager. The instrument will be incorporated into a 3U Colony 2 CubeSat bus provided by the National Reconnaissance Office for launch in late 2015 with mission duration > 8 months. Two critical science questions will be answered:

1. How much do geomagnetic storms alter the temperature structure of the lower thermosphere at low- and mid-latitudes?
2. What are the temperature signatures of internal atmospheric waves in the lower thermosphere?

The high-latitude region of the thermosphere responds promptly to energy inputs, relatively little is known about the global/regional response to these energy inputs. Global temperatures are predicted to respond within 3-6 hours, but the details of the thermal response of the atmosphere as energy transports away from their high-latitude source region is not well understood. This is the motivation of the OPAL mission to observe the temperature structure of the lower thermosphere at low- and mid-latitudes.

Wave coupling from lower to higher altitudes in the neutral atmosphere represents key additional pathways for the flow of energy and momentum into the thermosphere. A diverse spectrum of neutral atmospheric waves exists in the Mesosphere and Lower Thermosphere (MLT) region, excited mainly by solar inputs at lower altitudes, and manifest as solar tides, planetary waves and gravity waves. Together, these waves span a broad range of spatial and temporal scales and are believed to be the major drivers of the thermospheric variability under quiet solar and geomagnetic conditions. However, direct evidence for the penetration and effects of these waves on the thermal structure of the lower thermosphere and its variability is only just emerging. Within this paper we overview the mission and science objectives of OPAL.

Irregularities of Ionosphere or Atmosphere

IRRI-01 Occultation Scintillation Observed by FORMOSAT-3/COSMIC in 2007-2014 - by Chen, Shih-Ping

Status of First Author: Student IN poster competition, PhD

Authors: S. P. Chen, J. Y. Liu, Dieter Bilitza, W. H. Yeh

Abstract: Occultation radio scintillation of GPS L1-band (1.575GHz) has been recorded by FORMOSAT-3/COSMIC for over 7 years since 2007. Massive data (~4000 profiles daily) collected by six LEO satellites allow us to observe density irregularity distribution in 3D globally. With F3/C's high spatial and temporal resolution, especially upon the oceanic region that cannot be provided by ground-based observation, the F3/C scintillation data can be used as a powerful investigator of irregularity. In this presentation, a series of scintillation evolution from recently solar minimum (2009) to solar maximum (2014) will be shown in latitudinal/ diurnal/ seasonal, and solar activity variation.

IRRI-02 Alfvén waves in the ionosphere: cutoff altitude and feedback instability - by Cosgrove, Russell Bonner

Status of First Author: Non-student

Authors: Russell Cosgrove and Eugene Dao

Abstract: It is generally considered that magnetospherically generated electric fields are communicated to the ionosphere by Alfvén waves. However, there has been very little study of Alfvén waves in the ionosphere. Previous derivations of the Alfvén wave dispersion relation do not fully account for important collisional effects. In this work, the complete, fluid, linear dispersion relation for Alfvén waves, including the parallel electric field with electron-ion, ion-electron, ion-neutral, and electron-neutral collisions is derived. We find that the parallel electric field provides that, for a given frequency, there is a minimum perpendicular wavelength. The minimum perpendicular wavelength increases with decreasing altitude, such that propagating modes are cutoff, and become evanescent below a certain altitude. Electromagnetic simulations based on EMI are being prepared to test this result, and we give here preliminary results that show surprising effects related to the mapping of electromagnetic fields through the ionosphere, and to feedback from waves reflected from high altitudes.

IRRI-03 Acoustic Waves Detected in the F-region Ionosphere by the TIDDBIT HF TID Mapping System - by Crowley, Geoff

Status of First Author: Non-student

Authors: G. Crowley, R. L. Walterscheid, M. P. Hickey, J. H. Hecht

Abstract: We have performed a detailed analysis of data from a new Digital HF Doppler sounding system to estimate the propagation parameters of acoustic gravity waves in the F-region. This system, called the "TID Detector Built In Texas" (TIDDBIT) is formed by six HF continuous wave (CW) transmitters, and four digital receivers, and a digital data acquisition system. The system transmits HF radio waves at two frequencies, which are reflected from altitudes determined by the corresponding plasma frequency, and which vary during the day between altitudes ~ 200-400 km. The system records the Doppler shift due to the movement of the isoionic surfaces at 30 s intervals. A spectral analysis of the data from October 30, 2007, when the system was sited near Wallops Island, Virginia, shows strong spectral peaks in the acoustic range

in the period interval ~ 3-7 minutes. The power in this region shows a high degree of coherence between three transmission sites located ~ 50 – 100 km from the receiver. A wavelet analysis shows a sequence of discrete events occurring over the day in the 3-7 minute range. An analysis of the phasing between the three transmission sites indicates that horizontal trace speeds in this range are between ~ 500 and 800 m s⁻¹ with horizontal wavelengths between ~ 100 and 300 km. Calculations with a full-wave model indicate that the waves are consistent with internal acoustic waves with upward energy propagation. We conclude that significant acoustic disturbances occurred at F-region altitudes over the TIDDBIT array and that they are upward propagating waves originating below the F region, possibly from tropical storm Noel.

**IRRI-04 TID Observations at Middle and Low Latitudes Using the TIDDBIT HF
TID Mapper - by Crowley, Geoff**

Status of First Author: Non-student

Authors: G. Crowley, A. Reynolds, M. Milla

Abstract: HF Doppler sounders represent a low-cost and low-maintenance solution for monitoring wave activity in the F-region ionosphere. HF Doppler sounders together with modern data analysis techniques provide both horizontal and vertical TID velocities and wavelengths across the entire spectrum from periods of 1 min to over an hour. ASTRA has developed a new system called "TIDDBIT" (TID Detector Built In Texas), and data will be presented from TID mapping systems in Texas, Virginia, Peru and Antarctica. We show how the TIDDBIT data provides information on wind-filtering of gravity waves. The completeness of the wave information obtained from these systems makes it possible to reconstruct the vertical displacement of isoionic contours over the ~200 km horizontal dimension of the sounder array, which will be demonstrated with movies. A TIDDBIT Sounder has been deployed in Jicamarca, Peru for two years. Results from the Jicamarca site will be shown and compared with the sounder data from other locations. The TIDDBIT system in Peru detected atmospheric waves generated by the Japanese earthquake/tsunami in March 2011. Spread-F conditions detected by TIDDBIT are also compared with GPS scintillation detected by ASTRA's CASES dual-frequency receiver in Jicamarca. The Pre-Reversal Enhancement in vertical plasma drift causes the F-region ionosphere to rapidly increase in altitude, which is also measured by the TIDDBIT sounder in Peru.

**IRRI-05 OSSE Experiments to Determine the Value of Various Observing Systems
for Ionosphere-Thermosphere Specification - by Crowley, Geoff**

Status of First Author: Non-student

Authors: I. Azeem, G. Crowley, M. Pilinski

Abstract: Assessments of the relative value of various observing systems can be made using techniques called Observing System Simulation Experiments (OSSE's) and Observing System Evaluations (OSE's). OSEs are used to simulate the exclusion or loss of various existing instruments, platforms or missions. OSSEs are undertaken to quantitatively assess the relative value and benefits of future observing capabilities and systems, and should be conducted prior to the acquisition of major Government-owned observing systems, including polar-orbiting and geostationary satellite systems. Each of these techniques relies on the idea that data from various instruments can be assimilated to provide improved specifications of atmospheric parameters. However, the value of the various instrument types or their location on the ground or in space may not be immediately obvious. These tools provide quantitative assessments of the impact of various measurements on atmospheric specification, as defined by various metrics.

ASTRA is developing software tools to quantitatively assess the impact of various measurements for both ionospheric and thermospheric specification. These tools can simulate ionospheric plasma density and thermospheric density measurements (and the corresponding uncertainties) from in-situ and remote sensing space-based and ground-based sensors, and then ingest them using assimilation algorithms. In particular, they can aid our understanding of how much an existing or proposed observing system will improve the performance of data assimilation algorithms. The impact of the measurements can be quantitatively assessed as instruments are added or removed from the simulation.

The first tool, called Prediction of Ionospheric Observations and Nowcasting Errors with Emulation of Results (PIONEER), simulates sensor measurements of ionospheric electron density, and ingests them into a global ionospheric electron density assimilation algorithm. Current simulation capabilities for the ionosphere include ground-based GPS TEC, beacon receivers, vertical and oblique ionosondes, backscatter sounders, IS radars, space-based in-situ, UV remote sensing and GNSS radio occultation. The second tool called Simulator for Atmospheric Neutral Density Experiments (SANDE) is currently under development. It will simulate sensor measurements of thermospheric neutral density and assimilate them into a global model to assess their relative value.

The PIONEER and SANDE tools have been designed to provide full simulation of the spatial and temporal distribution of existing and planned sensors and the corresponding data and uncertainties. These tools provide the ability to perform quantitative assessments of the utility of existing and planned sensors for ionospheric and thermospheric density specification. ASTRA's OSSE/OSE tools are designed to be flexible so they can be used to examine the impact of observations on a particular application, or to give insight into their effectiveness in a data assimilation system.

In this paper, we will describe the system architecture for the PIONEER tool, and a case study to demonstrate its unique capability of performing assessments of the utility of existing and planned sensors for global and regional ionospheric specification for Space Situational Awareness. This kind of tool is vital for 'Analysis of Alternatives' exercises, and will help to maximize the utility of new sensors and ionospheric measurement systems, such as the planned COSMIC and other Radio Occultation missions. It could also save the government millions of dollars by preventing the purchase and deployment of unnecessary or redundant sensors that provide a low return on investment.

IRRI-06 Inverse modeling using a novel GPS scintillation model, SIGMA, to characterize high latitude irregularities - by Deshpande, Kshitija Bharat

Status of First Author: Student IN poster competition, PhD

Authors: Kshitija Deshpande, Gary Bust, C. Robert Clauer, Allan Weatherwax

Abstract: We have developed a high fidelity "Satellite-beacon Ionospheric-scintillation Global Model of the upper Atmosphere" (SIGMA) which is a full 3D EM wave propagation model to simulate GPS scintillations globally. We demonstrate in this work that the results from this model can form a basic framework on the use of inverse method to understand the physics of high latitude irregularities using GPS scintillations. We are using SIGMA and an inverse method to understand the physics of the irregularities observed with GPS receivers from six different inter-hemispheric high latitude stations on 9 March 2012. We also utilize ancillary observations from SuperDARN, ISRs, riometers etc. to obtain some of the input parameters of SIGMA. We implement a uniform-grid SIGMA simulation or a non-linear optimization of the model to obtain the rest of the unknowns that give us the best fit with data. The input parameters of SIGMA thus derived represent the physical and propagation parameters related to the physics of the irregularity that produced those GNSS scintillations. Some of our findings from this investigation include that the spectral indices and outer scales for ionospheric heights of 350 km are higher than those at 120 km. The best fits we obtained from our inverse method mostly agree with the observations except for some cases, which might be because the spectral model we use is insufficient to describe the irregularity physics.

We need more auxiliary data in order to facilitate the possibility of accomplishing a unique solution to the inverse problem.

IRRI-07 Identification of the generation source of decameter-scale ionospheric irregularities on plasmopause field lines - by Eltrass, Ahmed Said Hassan

Status of First Author: Student IN poster competition, PhD

Authors: A. Eltrass, W. A. Scales, A. Mahmoudian, S. de Larquier, J. M. Ruohoniemi, J. B. H. Baker, R. A. Greenwald, and P. J. Erickson

Abstract: The mid-latitude SuperDARN radars have revealed decameter-scale ionospheric irregularities during quiet geomagnetic periods that have been proposed to be responsible for the observed low-velocity Sub-Auroral Ionospheric Scatter (SAIS). The mechanism responsible for the growth of such common irregularities is still unknown. Joint measurements by Millstone Hill Incoherent Scatter Radar (ISR) and SuperDARN HF radar located at Wallops Island, Virginia reported by Greenwald et al. [2006] have determined decameter-scale irregularities with low drift velocities in the quiet-time mid-latitude night-side ionosphere. Temperature gradient instability (TGI) is investigated as the cause of irregularities associated with these SuperDARN echoes. The electrostatic dispersion relation for TGI has been extended into the kinetic regime appropriate for SuperDARN radar frequencies by including Landau damping, finite gyro-radius effects, and temperature anisotropy. This dispersion relation allows study of the TGI over a wide range of parameter regimes that have not been considered for such ionospheric applications up to this time. The calculations of electron temperature and density gradients in the direction perpendicular to the geomagnetic field have shown that the TGI growth is possible in the top-side F-region for the duration of the experiment. A time series for the growth rate has been developed for mid-latitude ionospheric irregularities observed by SuperDARN in the top-side F-region [Greenwald et al., 2006]. This time series is computed for both perpendicular and meridional density and temperature gradients. These observations show the role of TGI is dominant over the gradient drift instability (GDI) in this case. Nonlinear evolution of the TGI has been studied utilizing gyro-kinetic "Particle In Cell" (PIC) simulations with Monte Carlo collisions. This allows detailed study of saturation amplitude, particle flux, heat flux, diffusion coefficient, and thermal diffusivity of the resistive drift wave turbulence. The simulation results have been compared with the linear theory. The simulations show important consequences of nonlinear evolution, particularly saturation mechanisms and wave cascading of TGI into the decameter-scale regime of the radar observations. This result implies that the E-region may be responsible for shorting out the F-region TGI electric fields before and around sunset. A critical comparison of computational modeling results and experimental observations is discussed.

IRRI-08 A statistical investigation of decameter-scale plasma waves in the polar F region - by Lamarche, Leslie Jean

Status of First Author: Student IN poster competition, PhD

Authors: L. J. Lamarche and R. A. Makarevich

Abstract: We present a statistical study of F-region coherent echoes from the southern polar cap observed with the Super Dual Auroral Radar Network (SuperDARN) High Frequency (HF) radar at the McMurdo Antarctic station between 2010-2013. HF radars detect coherent echoes from ionospheric plasma waves of decameter scales and percentage occurrence estimates of these waves in the polar F region (altitudes above 150 km) were calculated for each latitudinal bin observed by the SuperDARN McMurdo radar. A band of high occurrence was found which changed its latitudinal position with universal time (UT) and season. A cosine function of UT was found to model the band reasonably well both in terms of band center position

and band width. The band width and amplitude of the cosine fit are shown to be consistently greater in winter months. In addition, the time of day when the occurrence band was farthest from the radar was found to be later in the winter than in the summer. Model results are interpreted in terms of solar zenith angle and plasma density variations with season and local time. In the second part of this study, the effects of Ultra Low Frequency (ULF) wave activity in the Interplanetary Magnetic Field (IMF) over plasma convection and ULF wave activity in the F-region ionosphere are investigated. Wavelet analysis was conducted on the radar-measured Doppler velocity at 1-min resolution for days with a high echo occurrence. Wavelet analysis was also performed on the IMF Bz and By components for the corresponding time period. The peaks in the wavelet spectra and their change over time were considered to determine strongest spectral contributions to the time series. Preliminary results based on two events are presented. Enhancements in the IMF wave activity are shown to be reflected in similar enhancements in the velocity wavelet spectra at corresponding times. Moreover, wave periods of strongest peaks in wavelet spectra of the IMF and convection velocity are found to be similar, as well as their variation with time. A relationship between the electric fields in the solar wind and in the polar cap is discussed.

IRRI-09 Observations of three dimensional spatial plasma structures of F region 3-m field-aligned irregularities made with Chung-Li VHF radar - by Lin, Fei-Fan

Status of First Author: Student IN poster competition, Undergraduate

Authors: C.L. Su, C.Y. Wang, Y.H. Chu

Abstract: Three-meter field-aligned irregularities (FAIs) occurred in nighttime F region at low latitude on 5 February 2008, 5 March 2011, 26 October 2012, 31 March 2014 and 19 March 2014 were observed by using the Chung-Li VHF radar. Interferometry measurements show that the plasma structures of the observed 3-m FAIs occurred in a height range of 250-350 km are in a quasi-isotropic blob shape with a dimension of about 25–50 km. Statistics indicate that the radial velocities of the F region 3-m FAIs are in a range of 220 – 320km height, corresponding to the zonal electric fields of -4.7–5.4 mV/m in the plasma structures. The zonal trace velocities of the plasma structures, which are obtained from their temporal displacements in the horizontal plane, are estimated to be -131m/s and 140 m/s, in which positive (negative) values indicate westward (eastward) drift. A comparison reveals that some of the F region 3-m FAIs observed by the Chung-Li radar at low latitude are closely related to those occurred at geomagnetic equator. However, the cases that the F region 3-m FAIs occurred over the Chung-Li radar site are independent of those over geomagnetic equator are also observed. The plausible causes of these different results are analyzed and investigated in this paper.

IRRI-10 GNSS scintillations in the nightside polar ionosphere over Svalbard - by van der Meeren, Christer

Status of First Author: Student IN poster competition, Masters

Authors: Christer van der Meeren, Kjellmar Oksavik, Dag Lorentzen

Abstract: In this poster we present preliminary results from a study of high-latitude irregularities and multi-constellation GNSS scintillations in the nightside ionosphere over Svalbard, possibly supplemented with data from incoherent and coherent scatter radars and optical ground-based instruments.

Scintillations are rapid amplitude and phase fluctuations of electromagnetic signals. GNSS-based systems may be disturbed by ionospheric plasma irregularities and structures such as plasma patches (areas of enhanced electron density in the polar cap) and plasma gradients. When the GNSS radio signals propagate through such areas, in particular gradients, the signals experience scintillations that at best increases

positioning errors and at worst may break the receiver's signal lock, potentially resulting in the GNSS receiver losing track of its position.

Due to the importance of many GNSS applications, it is desirable to study the scintillation environment to understand the limitations of the GNSS systems.

IRRI-11 Characteristics of 3-m field-aligned irregularities in daytime and nighttime sporadic E region made with Chung-Li VHF radar - by Wang, Chien-Ya

Status of First Author: Non-student

Authors: Chien Ya Wang

Abstract: With interferometry measurements made with Chung-Li VHF radar, statistics of the 3-m layer type field-aligned irregularities (FAI) are presented. Data include 27 days backscatter echoes which received in 2008-2009 February, May, July and October are used. Sporadic E layers occur in 0600~1800 LT (1800~0600) are defined as daytime (nighttime) echoes, there are 17 daytime echoes in this report. Analysis show that layers mean heights are at 92~105 (92~110 km) for daytime (nighttime), that is they have almost same lower bound but night echoes have about 5 km upper bound. The spectral moments show that mean Doppler velocities are ± 50 m/s (-60~90 m/s), whereas spectrum widths are 25~75 m/s (5~80 m/s) for layer echoes in daytime (nighttime). The layer thickness and zonal extent can be 0.1~4 km and 10~40 km for all the days. The field aligned angles are primarily in $0.2^\circ \sim 0.8^\circ$ ($0.1^\circ \sim 0.9^\circ$) for those day (night) echoes. Compare with the results in Wang et al. 2011, we find the height upper bound of nighttime layers at 110 km are almost the same, while the lower bound height down about 3 km in this report. Beside these, the largest spectral width has about one half of previous statistics.

IRRI-12 Three-dimensional high-resolution plasma bubble modeling - by Yokoyama, Tatsuhiro

Status of First Author: Non-student

Authors: Tatsuhiro Yokoyama, Hiroyuki Shinagawa, and Hidekatsu Jin

Abstract: Equatorial plasma bubble (EPB) is a well-known phenomenon in the equatorial ionospheric F region. As it causes severe scintillation in the amplitude and phase of radio signals, it is important to understand and forecast the occurrence of EPB from a space weather point of view. The development of EPB is known as a evolution of the generalized Rayleigh-Taylor instability. Numerical modelings of the instability on the equatorial two-dimensional plane have been conducted since the late 1970's, and the nonlinear evolution of the instability has been clearly presented. Recently, three-dimensional (3D) modelings became popular tools for further understanding of the development of EPB such as 3D structure of EPB, meridional wind effects and gravity wave seeding. One of the biggest advantages of the 3D model is that the off-equatorial E region which is coupled with the equatorial F region can be included in the model. It is known from observations that the conductance of the off-equatorial E region controls the growth rate of the Rayleigh-Taylor instability, that is, sudden decrease of the E-region conductance around the sunset accelerates the evolution of the instability. We have developed a new 3D high-resolution model for EPB. As it is necessary to use high-order numerical schemes to capture sharp plasma density gradient of EPB, we adopted the CIP scheme which can keep the third-order accuracy in time and space. We have successfully reproduced turbulent structures inside EPB and bifurcation at the top of EPB. In the future, we will integrate the high-resolution model into whole atmosphere-ionosphere coupled model (GAIA) to study the growth of EPB under the realistic background conditions.

IRRI-13 Applying the Fourier, Capon and Maximum Entropy Imaging Techniques to Sao Luis Coherent Radar Interferometer Measurements -
by Zewdie, Gebreab Kidanu

Status of First Author: Student IN poster competition, PhD

Authors: Gebreab K. Zewdie and Fabiano S. Rodrigues

Abstract: The interferometric radar imaging technique has been used to obtain two dimensional distribution of meter scale irregularities causing coherent scatter echoes (Kudeki et al, 1991; Hysell, 1996; Rodrigues et al, 2012; Harding et al, 2013). The Maximum entropy method (MEM) algorithm developed by Hysell (1996) has been used to obtain in-beam images from measurements made by the 30MHz Sao Luis radar interferometer (2.590 S, 44.210N; -2.350 dip lat), during two distinct equatorial spread F events (Rodrigues et al. , 2008; Rodrigues et al. 2012). In an attempt to optimize analysis and data visualization, we developed Matlab codes that use three distinct inversion approaches: Inverse Fourier Transform, Capon method (Palmer, 1998), and MEM (Hysell, 1996). On this workshop, we will present results of our inversion algorithms applied to different types of Equatorial Spread F (ESF) events observed by the Sao Luis radar interferometer.

IRRI-14 Nonthermal plasma modes in the terrestrial ionosphere - by Isham, Brett

Status of First Author: Non-student

Authors: Brett Isham, Vasyl Belyey, Patrick Guio, Jim LaBelle, C{\\e}sar La Hoz, Thomas Leyser.

Abstract: Nonthermal ion-acoustic and Langmuir modes are important to a variety of topics within the field of ionospheric and space physics. A number of mechanisms have been proposed to explain the origins of these nonthermal electrostatic modes. Although several of these mechanisms may be effective in enhancing one or both modes, only Langmuir turbulence is well-supported by both observations and modeling. We present observations by the EISCAT VHF (220 MHz) radar of the spectra of up- and down-going Langmuir and ion-acoustic waves at wave vectors of approximately 9 m^{-1} , including additional features of natural cavitating Langmuir turbulence, and show related modeling results. We conclude by discussing the current understanding of ionospheric Langmuir turbulence.

IRRI-15 Understanding the Response of the Ionosphere to Atmospheric Waves Generated by Tsunamis and Other Geophysical Disturbances -
by Drob, Douglas Patrick

Status of First Author: Non-student

Authors: Douglas P. Drob¹ and J. D. Huba²

1) Space Science Division, Naval Research Laboratory, Washington DC, USA

2) Plasma Physics Division, Naval Research Laboratory, Washington DC, USA

Abstract: We present results from the coupling of the ground-to-space atmospheric spectral gravity wave model of Drob et al., (2012) with the SAMI3/ESF first-principles ionosphere model of Huba et al., (2009). This coupled physics-based simulation capability provides a means to explore, understand, and characterize the various factors that determine the response of the ionosphere to atmospheric gravity waves generated by tsunamis and other geophysical seismo-acoustic phenomena. These factors include; 1) the wavelength,

frequency content, and propagation direction of the ocean/ground motion; 2) the seasonal and geographic factors which determined the anisotropic atmospheric background wind filtering and thermospheric gravity-wave dissipation processes; 3) the seasonal, geographic, local-time, and solar flux conditions that determine the background electron density and ionosphere conductivity profiles; and 4) the relationship of the atmospheric perturbations with respect to the geomagnetic field. For example, by comparing the results of simulations with and without gravity wave-perturbations we explore the effect of zonal, meridional, and vertical gravity wave wind perturbations across a range of geomagnetic latitudes (and thus geomagnetic pitch angle) to the resulting plasma velocity perturbations along the corresponding geomagnetic fields lines, as well as to the subsequent perturbations of total electron content (TEC). For comparable atmospheric gravity wave amplitudes, we find TEC variations of $\sim \pm 0.1$ TECU (1 TECU = 10¹⁶ m²) which are consistent with observations made during the 11 March 2001 tsunami. This work sponsored by the Office of Naval Research.

Long Term Variations of the Ionosphere-Thermosphere

LTVI-01 Solar Zenith Angle as a Driver of Seasonal Oscillations in the Ionosphere - by Hawkins, Jessica

Status of First Author: Student IN poster competition, Masters

Authors: Jessica M. Hawkins and Phillip C. Anderson

Abstract: The path that solar radiation takes through the Earth's atmosphere varies over the course of a year due to the changing solar zenith angle, and this is a significant driver of changes in ionospheric density. Solar zenith angle (SZA) effects show up in measurements of ion density as a seasonal oscillation which is approximately sinusoidal. It may be desirable to remove the SZA effects from ion density data in order to focus on other variables affecting the ionosphere, and one method that can be used to remove the SZA oscillation is Empirical Orthogonal Function (EOF) analysis. We perform EOF analysis on DMSP satellite data and show that projections onto the first two EOFs correlate strongly with solar EUV irradiance and SZA, indicating that these two variables explain most of the variance. We then explain how to create a revised data set, using EOF analysis to remove SZA effects, and we show that the revised data has a stronger correlation with solar EUV than the un-revised data.

LTVI-02 Thermospheric hydrogen response to increases in greenhouse gases - by Nossal, Susan Marcelle

Status of First Author: Non-student

Authors: S.M. Nossal, L. Qian, S. Solomon, W. Wang, A. Burns, F.L. Roesler, E.J. Mierkeiwicz, R.C. Woodward

Abstract: Sensitivity studies with the NCAR Global Mean Model, a single column version of the Thermosphere Ionosphere Mesosphere Electrodynamics General Circulation Model, predict that rises in both carbon dioxide and methane result in an increase in the upper thermospheric atomic hydrogen density. There is also predicted to be a solar cycle influence on this response to greenhouse gas changes. We will discuss mechanisms for the solar cycle impact, and for source species increases and carbon dioxide cooling upon hydrogen-containing species distributions, including the role of the upper boundary hydrogen escape flux. The apparent upward trend in the Wisconsin hydrogen emission data set is of greater magnitude than would be predicted from increases in greenhouse gases. We will also discuss work in progress to investigate whether this trend is geophysical or an artifact of the calibration or analysis.

Magnetosphere-Ionosphere-Thermosphere Coupling

MITC-01 Relationships between Birkeland current onset dynamics and IMF/solar wind forcing - by Anderson, Brian J.

Status of First Author: Non-student

Authors: Brian J. Anderson, Haje Korth, Colin L. Waters, Ethan S. Miller, Lawrence J. Zanetti, and Robin J. Barnes

Abstract: Development of Birkeland currents are monitored using AMPERE observations for clear signatures of current onsets that are isolated from prior activity by at least one hour. In examples, the response to onset of southward IMF is that poleward (R1) and equatorward (R2) currents develop together first on the dayside and then together starting near midnight with subsequent expansion and intensification toward the dayside. This suggests that dayside reconnection drives anti-sunward flows near noon and a modest R1/R2 system develops promptly whereas only later, with the onset of magnetospheric return flows and plasma injection into the inner magnetosphere, do the R2 currents develop beginning near midnight and this simultaneously promotes R1 currents paired with these new R2 currents. In this study, we examine onsets of currents in AMPERE data systematically to establish the relationships of the time sequence of dayside/nightside and Region 1/Region 2 to the time history of IMF/solar wind forcing. We address the following questions: How prevalent is the day-to-night sequence evident in the examples? How isolated does the onset need to be to exhibit this behavior? Does a magnetosphere already populated with inner magnetospheric plasmas display the same day-night delay or is the response of R1/R2 more instantaneous? How does the sequence of Birkeland current and convection electric field progress under strong IMF BY conditions?

MITC-02 Aspect-angle dependence study of naturally enhanced ion-acoustic lines - by Akbari, Hassanali

Status of First Author: Student IN poster competition, PhD

Authors: Hassanali Akbari, Joshua Semeter

Abstract: The aspect-angle dependence of naturally enhanced ion acoustic lines (NEIALs) is investigated using two multi-beam experiments with the electronically steerable Poker Flat incoherent scatter radar (PFISR). Two types of echoes with different characteristics are studied that are consistent with parametric decay and ion-ion streaming instabilities, respectively. While dynamics of auroral activity suggests that the source of the echoes, whether it is electron beam or field-aligned current, is equally present, in a statistical sense, in a wide portion of sky, strong variations in intensity of NEIALs is observed when radar beam direction is altered by only one degree. In the both types of echoes the strongest scattered power appears in the magnetic-zenith beam and weakens as the angle of the radar beam increases with respect to magnetic field lines. This dependency is more intense for the echoes that are produced by streaming instability and is yet much more critical for higher altitude (> 250 km) NEIALs than for lower altitude ones (< 200 km). Whether this later is due to a different generation mechanism for lower altitude NEIALs or due to parameters of the ambient plasma is not known. Results presented here are specifically surprising since previous experiments have successfully detected NEIALs at large aspect angles, up to 15 degrees.

MITC-03 Electron Energy Dispersion as seen by the ePOP Suprathermal Electron Imager - by Cameron, Taylor

Status of First Author: Student IN poster competition, Masters

Authors: Taylor Cameron, David Knudsen, Johnathan Burchill

Abstract: The ePOP Suprathermal Electron Imager (SEI) records 2D electron energy distributions on the range 5-350 eV at a rate of 100 per second. We have searched data from the first few months of operation of this instrument for signs of electron energy dispersion, and have identified examples of both ordinary and inverse electron dispersion of relatively cold electron populations, and also sub-visual, < 400 eV inverted-V signatures characterized by hotter electrons. In this poster, we will present examples of these phenomena, and argue that inverse dispersion of cold electrons is a spatial effect resulting from a broad-spectrum electron beam drifting relative to background plasma.

MITC-04 Initial results of storm-time IT responses using the OpenGGCM-CTIM global magnetosphere-ionosphere-thermosphere model - by Connor, Hyunju

Status of First Author: Non-student

Authors: M. Fedrizzi, E. Zesta, T. Fuller-Rowell, J. Raeder

Abstract: During a geomagnetic storm, the ionosphere – thermosphere (IT) system is strongly affected by auroral particle precipitation and high-latitude ionospheric electric fields. The role of these magnetospheric energy inputs on the IT system is not yet fully understood due to a lack of simultaneous satellite and ground observations covering the entire polar region. Many of the physics-based IT models applied to the problem depend on empirically-calculated magnetospheric energy inputs, such as Weimer’s potential patterns and the NOAA/TIROS statistical auroral map, so the models do not sufficiently capture storm dynamics. To improve prediction of the storm-time IT response, a physics-based magnetospheric energy input is needed. We present initial modeling results of a geomagnetic storm on Aug 24, 2005 using OpenGGCM-CTIM, the two-way coupled global magnetosphere-ionosphere-thermosphere (MIT) model. The OpenGGCM magnetosphere-ionosphere model provides physics-based calculations of auroral precipitation and ionospheric electric fields to the CTIM ionosphere-thermosphere model. Then, CTIM provides realistic Hall and Pederson conductivities back to the OpenGGCM to improve electric field prediction during the next time step. We also present IT-only model results for the same storm by using empirically calculated magnetospheric energy as input to CTIPe, the latest version of the CTIM model. Comparison of the two model results with the neutral density data of CHAMP and GRACE shows that the MIT model provides an improved storm-time IT response by reproducing a strong enhancement of neutral densities in the high-latitude regions during the early phase of a geomagnetic storm.

MITC-05 Investigation of EMIC Wave Scattering as the Cause for the BARREL January 17, 2013 Relativistic Electron Precipitation Event - by Li, Zan

Status of First Author: Student NOT in poster competition, PhD

Authors: Zan Li, Robyn Millan, Mary Hudson, Leslie Woodger, Yue Chen, Reiner Friedel, Juan Rodriguez, Jerry Goldstein, Joseph Fennell, Mark Engebretson and Harlan Spence

Abstract: Abstract A duskside relativistic electron precipitation (REP) event observed during the BARREL first campaign on Jan 17, 2013 was in conjunction with electromagnetic ion cyclotron (EMIC) waves observed by the GOES-13 satellite. We simulate the relativistic electron pitch-angle diffusion caused by gyroresonant interaction with EMIC waves using wave and particle data measured by multiple instruments onboard of GOES-13 and the Van Allen Probes, and quantitatively compare the energy distribution of the resulting precipitation with BARREL spectrometer data. We show that, consistent with the quasi-linear simulation, the measured REP energy spectrum gets harder with time, but the time it took for the precipitation to reach its peak was observed to be much longer. In addition, a high level of low

energy precipitation was simultaneously detected, suggesting that the REP event cannot be explained by EMIC waves alone.

MITC-06 A Cubesat Instrumentation Suite for In-Situ Measurements of Wave-Induced Particle Precipitation - by Sousa, Austin Patrick

Status of First Author: Student IN poster competition, PhD

Authors: Austin Sousa, Steven Ingram, Christopher Young, Dr. Robert Marshall, Dr. Ivan Linscott, Dr. Jack Doolittle, Dr. Robert Bumala, Dr. Umran Inan

Abstract: The VLF Wave/Particle Precipitation Mapper (VPM) is a 1.5-unit Cubesat payload, designed by the Stanford VLF group in conjunction with Lockheed Martin, which will make direct measurements of energetic particle precipitation due to incident ELF/VLF electromagnetic waves. Herein we present an overview of the payload design, including performance characteristics and its intended modes of operation. Incident waves are measured by electric dipole antenna and a magnetic field search coil connected to a low-noise VLF radioreceiver; particle fluxes are measured using two electron energy spectrometers, one inside and the other outside the loss-cone. A Data Processing Unit provides two modes of operation: a low-resolution survey mode, and a programmable burst mode, capable of sampling up to a minute of full-resolution data. Timing and position are provided by an onboard GPS receiver. In effort to achieve high reliability, the payload makes use of radiation-tolerant components and does not rely on any stored programming. The payload is in the final stages of design, and is due to launch in 2016.

MITC-07 Van Allen Probes Overview and New Resources available via the Mission Gateway by Mauk, Barry

Status of First Author: Non-Student

MidLatitude Thermosphere or Ionosphere

MDIT-01 Self-consistent generation of medium-scale traveling ionospheric disturbances (MSTIDs) within the SAMI3 numerical model - by Duly, Timothy

Status of First Author: Student IN poster competition, PhD

Authors: Timothy M. Duly, Joseph D. Huba, and Jonathan J. Makela

Abstract: Nighttime, electrified, medium-scale traveling ionospheric disturbances (MSTIDs) are a mid-latitude instability characterized by banded structures of unstable vertical displacements of electron density. Here, we investigate the development of MSTIDs within the SAMI3 (Sami3 is Another Model of the Ionosphere) wedge model. The numerical model includes a potential solver, which is crucial for the self-consistent generation of MSTIDs. These are the first numerical modeling results that use a full magnetic flux tube grid to show the MSTID signature in the conjugate hemisphere. We present synthetic observations of MSTIDs calculated within SAMI3, including total electron content (TEC), 630.0-nm airglow emission, electron density, and $E \times B$ drifts.

MDIT-02 pyglow: Upper atmosphere climatological models in Python -
by Duly, Timothy

Status of First Author: Student NOT in poster competition, PhD

Authors: Timothy M. Duly

Abstract: Climatological numerical models (e.g., IGRF, IRI, MSIS, HWM93/07) are commonly written in FORTRAN, and are often used within the upper atmosphere research community for a wide variety of applications (e.g., initializing values in numerical models and for comparisons against measured data). Here we present pyglow, a Python module that includes wrappers for climatological models. In this way, the climatological models can be accessed in the high-level and scriptable Python programming language. This implementation provides quick access to each model under a common framework. Pyglow is open-sourced (<https://github.com/timduly4/pyglow/>) to encourage improvement and expansion of the code base.

MDIT-03 Sources and Characteristics of Medium Scale Traveling Ionospheric
Disturbances Observed by a Longitudinally Distributed Chain of
SuperDARN Radars Across the United States -
by Frissell, Nathaniel Anthony

Status of First Author: Student IN poster competition, PhD

Authors: N.A. Frissell, J.B.H. Baker, J.M. Ruohoniemi, A.J. Gerrard, E.S. Miller, W.A. Bristow, and M.L. West

Abstract: Medium Scale Traveling Ionospheric Disturbances (MSTIDs) are wave-like perturbations of the F-region ionosphere with horizontal wavelengths on the order of 100-250 km and periods between ~15 - 60 min. In SuperDARN data, MSTID signatures are manifested as quasi-periodic enhancements of ground scatter power moving through the radar FOV. High latitude SuperDARN MSTIDs have been studied for many years and are generally attributed to atmospheric gravity waves (AGWs) launched by auroral sources. Recent extension of the SuperDARN network to midlatitudes has revealed that MSTIDs are routinely observed at midlatitudes as well. Our previous research using the single radar in Blackstone, Virginia found a primary MSTID propagation direction which suggests that high latitude activity is also the primary source of midlatitude MSTIDs. However, there is also a population of MSTIDs that could be generated by tropospheric sources. This study extends this research by surveying multiple midlatitude radars in Oregon (CVW and CVE), Kansas (FHW and FHW) and Virginia (BKS and WAL) from 1 November 2012 through 1 January 2013 for MSTID signatures in order understand the longitudinal distribution of midlatitude MSTID characteristics and understand possible influences of varied terrain on MSTID observations. MSTIDs observed by all radars had typical wavelengths between 250 to 500 km and horizontal velocities between 100 and 250 m/s. In all radars, the dominant population of MSTIDs propagated in a southward direction, ranging from 135° to 250° geographic azimuth. The dominant southward propagation direction suggests auroral sources are the dominant source of MSTIDs observed by SuperDARN radars at midlatitudes, which reinforces findings regarding the primary population in previous work.

MDIT-04 Model simulation of electron density profile in lower part of ionosphere -
by Lin, Yen-Chieh

Status of First Author: Student NOT in poster competition, PhD

Authors: Yen-Chieh Lin, Yen-Hsyang Chu

Abstract: Solar extreme ultraviolet radiation (EUV) and x rays can ionize the N₂, O, O₂, N and NO compositions of thermosphere. These photos collide with neutral gas produce the plasma (ions and electrons) of ionosphere as well as leads to dissociative ionization and dissociation of molecular species. For long, the EUVAC and HFG solar proxy model have been used to model daily solar irradiance flux by inputting F10.7 and F10.7A indexes. However, few studies have reported on using SDO-EVE as solar flux inputs when modeling ionospheric electron density. The aim of this study is to compare modeled electron densities between these three solar irradiance sources. In this study, ions and electron densities in E-& lower F1-region ionosphere are simulated by taking account of chemical reactions between eight ion (O+(4S), O+ (2D), O+ (2P), O₂⁺, N₂⁺, N⁺, NO⁺, Fe⁺) and five neutral composition (O, O₂, N₂, N, NO) as well as photoionization, photoelectron production of each neutral composition. Results indicated that SDO-EVE have great capacity to be as solar irradiance driver since the excellent spectral resolution and temporal cadence.

MDIT-05 Magnetic meridional winds in the thermosphere derived from GAIM and their sensitivity to atmospheric model parameters -
by Lomidze, Levan

Status of First Author: Student IN poster competition, PhD

Authors: Levan Lomidze and Ludger Scherliess

Abstract: Thermospheric neutral winds play an important part in the variations of ionospheric plasma at various temporal and spatial scales, and represent one of the key inputs for ionospheric physics-based models. Yet, available wind data is scarce because wind measurements lack the global coverage and continuity, and existing wind models need further improvements. To mitigate this shortcoming, a data assimilation model is used to estimate neutral winds in the low- and mid-latitude thermosphere simultaneously with the ionospheric electron density and the low-latitude electric fields. The assimilated data are seasonally averaged global maps of NmF₂ and hmF₂ generated from COSMIC GPS radio occultation measurements for geomagnetically quiet and low solar flux conditions. The COSMIC maps are assimilated into the Utah State University Global Assimilation of Ionospheric Measurements (USU-GAIM) model. The model uses a physics-based Ionosphere Plasmasphere Model (IPM) and employs an ensemble Kalman Filter technique. In the present work, global magnetic meridional winds in the thermosphere are derived for three different seasons. To validate the results, the estimated winds are compared with those from FPI measurements and with wind estimations from the empirical HWM93 model. In addition, the sensitivity of the derived wind velocity to uncertainties in the O⁺-O collision cross section and the thermospheric neutral composition is investigated. The analysis shows that uncertainties in these parameters are more important for nighttime winds over the mid-latitudes. The Results of this work indicate that thermospheric wind estimation from the ionospheric data assimilation model is a valuable tool for wind specification over regions where limited or no wind measurements exist. The derived winds, when used in IPM instead of the empirical HWM93 wind model, significantly improve the agreement between the modeled and measured electron densities in the ionosphere.

MDIT-06 High Altitude Acoustic Wave Generated by Launch of the Cygnus ORB-1 Mission to the ISS - by Mabie, Justin J.E.

Status of First Author: Student IN poster competition, PhD

Authors: Justin Mabie, Terrence Bullett

Abstract: A high altitude acoustic wave is observed in the Ionospheric F-layer after launch of the Cygnus Antares rocket at the NASA Wallops Flight Facility. The observation is made with the co-located

Vertically Incident Pulsed Ionospheric Radar (VIPIR) approximately 8 minutes after launch, consistent with observations of acoustic waves generated from Earthquakes and Tsunami's.

MDIT-07 MatLab Implementation for Ionosphere Modeling Using B-Spline, VTEC and IRI2012 Models - by Perez Ramirez, Freddy M.

Status of First Author: Student NOT in poster competition, PhD

Authors: Freddy Perez Ramirez, Jonathan Friedman

Abstract: The Ionosphere complexity has been matter of several studies with different approaches. Usually these models are empirical models used for modeling electromagnetic waves propagation and vertical structure for E and F Ionosphere regions. The conditions for the modeling go from calm conditions up to turbulence conditions. Due that the models are empirical there are discrepancies with the results. The International Reference Ionosphere (IRI) is a international project, is working in a global model of Ionosphere. These models are updated all the time. The updates are made using the data source of the powerful incoherent scatter radars (Arecibo Observatory, Jicamarca, Millstone Hill, Malvern, and St. Santin), and from the top sounders (ISIS and Alouette) between others. This work present a MatLab implementation for the B-spline, VTEC and IRI2012 models. The user can run these models in only one application. The IRI model parameters B0 and B1, are very important in this model. The goodness and performance of the model depends of the parameters accuracy.

MDIT-08 Magnetically Conjugate Observations of Ionospheric Processes Using All-Sky Imagers in the American Sector - by Sullivan, Catherine

Status of First Author: Student IN poster competition, Undergraduate

Authors: C.Sullivan, C.Martinis, R. Macinnis, M.Mendillo, J. Wroten, J. Baumgardner: CSP, BU
T. Moffat-Griffin: British Antarctic Survey, M. Taylor: Utah State University

Abstract: The Imaging Group at Boston University's Center for Space Physics (CSP) uses all-sky imagers (ASIs) across the globe to study ionospheric processes through the observation of 630.0 nm airglow patterns. Data from ASIs located in the American sector near the 75° geographic meridian are presented in the context of magnetically conjugate observations. At low and middle latitudes, ASIs at Arecibo, Puerto Rico (18.3°N, 66.7°W, 28° mag lat) and Mercedes, Argentina (34.7°S, 59.4°W, -25° mag lat) show signatures of equatorial spread F (ESF) and medium scale traveling ionospheric disturbances (MSTIDs). At higher latitudes, the ASIs at Millstone Hill, MA (42.6°N, 71.5°W, 51.8° mag lat), Rothera, Antarctica (67.6°S, 68.1°W, -52.6° mag lat), conjugate to Millstone Hill, and Rio Grande, Argentina (53.8°S, 67.7°W, -35° mag lat), are used to investigate the occurrence of Stable Auroral Red (SAR) arcs. Seen as a bright arcs poleward from the diffuse aurora and extended zonally along L shell values ~ 3 , they move equatorward and can reach lower mid-latitudes. Even though the three phenomena discussed here, ESF, MSTIDs, and SAR arcs, display, in general, excellent magnetic conjugacy, there are differences that can be related to local background conditions, meridional neutral winds, and how energy from the ring current is reaching sub-auroral latitudes.

**MDIT-09 Simulating electron and ion temperatures in Global Ionosphere
Thermosphere Model - by Zhu, Jie**

Status of First Author: Student IN poster competition, Masters

Authors: Jie Zhu and Aaron J. Ridley

Abstract: The electron temperature in the ionosphere is of great significance because it controls the rates of many physical and chemistry ionospheric and thermospheric processes. Simulating the electron temperature distribution in a global ionosphere thermosphere model requires including various heating, cooling processes, as well as thermal conduction. In this study, we implement the electron and ion energy conservation equations in a more self-consistent way in the Global Ionosphere Thermosphere Model (GITM). The electrons gain energy from photoelectrons and lose energy due to elastic and inelastic collisions with ions and neutrals. The ions gain energy by collision with thermal electrons and Joule heating, and lose energy to cool neutrals. The seasonal, latitudinal and UT dependence of the electron and ion temperature will be investigated. In low- and mid-latitudes, T_e shows a diurnal variation pattern with morning and evening peaks. In high latitudes, T_e is greatly influenced by downward electron heat flux from the magnetosphere. This study will also explore how the magnitude of downward heat flux affects the high-latitude ionosphere.

**MDIT-10 Observations of semidiurnal tidal variability at seasonal and day-to-day
time scales from the Boulder Fabry-Perot Interferometer -
by Chien, Shih Han**

Status of First Author: Student IN poster competition, Masters

Authors: Justin S.H. Chien, Loren C. Chang, Qian Wu, Charles C.H. Lin
1 Department of Earth Sciences, National Cheng Kung University, Tainan, Taiwan

Abstract: Atmospheric tides are a persistent feature of the mesosphere and lower thermosphere region, whose variability on seasonal and day to day time scales have important impacts on middle and upper atmosphere dynamics. The semidiurnal (12 hour period) tide is known to dominate MLT wind fields in the mid-latitude region, and has been found in past modeling studies to be important in controlling the ionospheric E-region wind dynamo, responsible for forming the Equatorial Ionization Anomalies (EIAs). Semidiurnal tidal features have been examined in the MLT from nighttime Fabry-Perot Interferometer (FPI) wind data over Boulder, Colorado in 2012 March to December on both seasonal and day to day time scales. Our sampling analysis shows that incomplete local time sampling can potentially result in contamination of FPI derived semidiurnal tidal amplitudes by the terdiurnal tide. However, the seasonal variation of our derived semidiurnal tidal amplitudes are consistent with the known variation of the semidiurnal tide, and inconsistent with those of the terdiurnal tide, suggesting that such contamination is not a major issue. Short-term anomalies in the total electron content (TEC) in the EIA region from global ionosphere maps are compared to anomalies in our FPI-derived semidiurnal tidal amplitudes, as well as changes in various geophysical indices to quantify their impacts on short-term EIA variability.

**MDIT-11 A study of the correlation between the midnight temperature maximum
signature and the total electron content in the mid-eastern continental
United States - by Mesquita, Rafael**

Status of First Author: Student IN poster competition, Masters

Authors: R. Mesquita, J. Meriwether, S. Sanders, J. Makela, D. Fisher, and B. Harding

Abstract: In this work, we present Fabry-Perot interferometer (FPI) thermospheric temperature and wind measurements that show the latitudinal distribution of the midnight temperature maximum (MTM) in the continental mid-eastern US. These results were obtained through simultaneous operation of the North American Thermosphere Ionosphere Observing Network (NATION) with the five FPI sites located at the Pisgah Astronomic Research Institute (PARI) (35.2° N, 82.8°W), Virginia Tech (VTI) (37.2° N, 80.4° W), Eastern Kentucky University (EKU) (37.8° N 84.3°W), Urbana-Champaign (UAO) (40.1° N 88.2°W) and Ann Arbor (ANN) (42.3° N 83.8°W). These results show the MTM structure varies from night to night with no significant MTM feature appearing on many of the nights in the NATION database. The MTM phenomenon is believed to be the result of the blending together of the upward propagating diurnal, semi-diurnal, and other higher order tidal modes. The amplitudes of these higher order waves increase in strength with height, until they become dissipated through the tidal wave interaction with the increased plasma densities in the E and F regions. Therefore, the FPI detection of the MTM perturbations in temperature and horizontal wind fields may depend on how much the upward propagating wave is dissipated due to the increased plasma densities before the wave reaches the 630-nm airglow layer near ~250 km. We present a statistical analysis of the MTM occurrence and compare these results with the results seen in examining total electron content (TEC) data as well as the available Millstone Hill incoherent scatter radar observations.

MDIT-12 A multi-instrument study of the vertical plasma drift difference associated with the pre-midnight brightness wave signature over the north-eastern Brazilian region - by Mesquita, Rafael

Status of First Author: Student NOT in poster competition, Masters

Authors: R. Mesquita, J. Meriwether, J. Makela, R. Buriti, I. Paulino, A. Fragoso, I. Batista, C. Alexandre, D. Fisher and S. Sanders.

Abstract: In this work, we present all-sky images obtained on two nights exhibiting the development of the pre-midnight brightness wave (PMBW) signature of enhanced 630-nm equatorial nightglow over the Cajazeiras (geographic: 6.87°S, 38.56°W; geomagnetic: 0.53°S, 33.29°E) and Sao Joao do Cariri (geographic: 7.38°S, 36.53°W; geomagnetic: 0.75°N, 35.43°E) airglow observatories located in north-eastern Brazil. The 630-nm all-sky images were obtained with the simultaneous operation of the INPE ionosondes at Cariri and the University of Illinois PICASSO/RENOIR imager at Cajazeiras. The PMBW signature was observed on the nights of 25 and 26 October 2011. Coincident observations of the thermospheric wind and temperatures were made with the RENOIR Fabry-Perot interferometers operating at both sites. CADI measurements obtained at Cariri, and the ionosonde measurements from Eusebio (geographic: 3.00°S, 45.00°W; geomagnetic: 5.84°N, 27.41°E) and Cachoeira Paulista (geographic: 22.70°S, 45.00°W; geomagnetic: 13.68°S, 25.84°E) are also available and were used to establish the virtual height of the F-layer's plasma. The downward plasma drift was calculated from the first time derivative of the F-layer's virtual height. These results demonstrate a strong correlation between the enhanced 630-nm nightglow intensity and the decrease of the F-layer's height during the PMBW event. We also show that the 630-nm nightglow intensity exhibits a PMBW signature going northward before midnight. The conclusion reached from the examination of these results is that the PMBW signature is caused by the early-evening downward plasma motion along the flux tube from the southern Appleton anomaly toward the geomagnetic equator. This behavior represents the nighttime plasma recovery from the geomagnetic storm transport of plasma toward southern latitudes. To look for confirmation of this conclusion, the ionosonde data is used to search for a possible connection between the appearance of the PMBW and the latitudinal dependence of the downward plasma drift rate observed near the geomagnetic equator and at sites located further toward the south.

Polar Aeronomy

POLA-01 Ion Thermalization at 500 km - by Archer, William

Status of First Author: Student IN poster competition, PhD

Authors: William Archer, David Knudsen, Johnathan Burchill

Abstract: The Electric Field Instruments (EFIs) aboard the Swarm satellites carry a new generation of thermal ion detector. A pair of these detectors mounted perpendicular to one another aboard each of the three satellites measure the local three dimensional ion velocity distribution. The EFIs primary function on Swarm is to measure local electric fields to provide corrections for magnetometer measurements being made on the satellites, however their design also makes them ideal for measuring ion temperature anisotropies.

For the first six weeks of the Swarm mission (launched in November 2013) the three satellites were in similar polar orbits, with satellites spaced 60 and 90 seconds apart. This configuration is ideal for measuring temporal variations in plasma conditions as all three satellites pass through the same regions. This study will focus on temperature anisotropy and temporal evolution of heated ions measured by the Swarm satellites at 500 km altitude.

POLA-02 Coupling of Low Altitude Ionospheric Upflow Processes to Ion Outflow - by Burleigh, Meghan

Status of First Author: Student IN poster competition, PhD

Authors: Matthew Zettergren

Abstract: Significant amounts of thermal ionospheric plasma can be transported to high altitudes in response to electron precipitation, frictional heating and neutral winds. In these high altitude regions, transverse ion acceleration is thought to give upflowing ions sufficient energy to outflow to the magnetosphere. This study examines the coupling of low altitude ion upflow processes with transverse ion energization. We focus specifically on how lower ionosphere dynamics feed transverse energization and determine the types, and amounts, of outflowing ions. A new 2D dynamic ionospheric simulation has been developed which encapsulates the basic ionospheric upflow responses and transverse heating effects. It consists of a set of equations describing the evolution of the mass, momentum, parallel and perpendicular energy of all species relevant to the E, F, and topside ionospheric regions. This fluid system is closed through an electrostatic treatment of the auroral currents and includes an ad hoc resonant heating term to describe transverse energization. Using this model the species response characteristics of lower ionosphere dynamics coupled with transverse energization are examined. This includes the driving effects of frictional heating and electron precipitation on ion upflow that creates the source populations for transverse energization and result in ion outflow. Neutral wind influences on these upflow characteristics are investigated as well. The results are compared against existing models.

POLA-03 Localized Ionospheric Cubeswarm Concept - by Clayton, Robert

Status of First Author: Student NOT in poster competition, PhD

Authors: Robert Clayton, Kristina Lynch, Dartmouth GreenCube group

Abstract: In interesting and dynamic auroral ionospheric plasmas, a localized array of sensors deployed as a low-resource swarm from a main deployer is enabled by the low resource aspect of small satellites and

resolve spatial and temporal differences. Thus a swarm of sensors can help understand the underlying truth of auroral dynamics more effectively than a single sensor.

In preparation for this, several sounding rocket based missions are deploying telemetered payloads complete with sensors to measure ion density gradients in the auroral ionosphere as well as develop the required hardware and software for an orbital swarm. Telemetered ground deploys of our ampules were conducted at Wallops Flight Facility and sounding rocket missions (Rosanova 46.007 and ISINGLASS) will launch out of Wallops and Poker Flat Research Range respectively. The results of these missions will provide science data similar to what a localized orbital cubesat swarm would be sending, and will allow for both the development of the payloads for the swarm and for the required data assimilation techniques to interpret the swarm of sensors present. The Rosanova flight also acts as a test flight for the ISINGLASS science mission, which provides several case studies of the auroral ionosphere.

In further progress towards a low resource orbital swarm of small sensors, a TeamXc design study was conducted at the Jet Propulsion Lab during March 2014 where the GreenCube group worked with JPL engineers to design a feasible orbital swarm point design including manufacturing, launch, deployment, orbital dynamics, attitude control, telemetry, and ground stations.

POLA-04 Sondrestrom Joule Heating Estimates - by Emery, Barbara

Status of First Author: Non-student

Authors: Barbara Emery (HAO/NCAR), Arthur Richmond (HAO/NCAR), Anja Stromme (SRI International), J Michael Ruohoniemi (VT)

Abstract: The Sondrestrom Fjord incoherent scatter radar calculates the Joule heat per unit volume as a function of height in the lower thermosphere using the MSIS model to estimate the neutral composition and temperature. The Joule heat per unit volume peaks in the E region near the peak of the Pedersen conductivity. We repeat the calculation of the Joule heat per unit volume, and expand our calculations to estimate the Joule heat per unit mass using only the observed electric fields. The Joule heat per unit mass peaks in the F-region near the peak of the electron density. We present our Sondrestrom Joule heat estimates for several storm periods and compare them to estimates from the Thermosphere-Ionosphere-Electrodynamics General Circulation (TIEGCM) model.

POLA-05 Simulations of the high-latitude ionosphere response to the 25 Feb 2014 X4.9-class solar flare - by Fallen, Christopher Thomas

Status of First Author: Non-student

Authors: William A. Bristow, Michel J. Nicolls

Abstract: An X4.9-class solar flare event began at approximately 00:41 hours UTC on 25 February 2014, causing extensive dayside high-frequency (HF) radar and communication blackouts. A flare is classified as X-class when the peak solar irradiance between 0.1 and 0.8 nm wavelengths (soft X-rays) at Earth exceeds $1e-4$ W/m², an enhancement of approximately two orders of magnitude greater than the typical irradiance. GOES satellite measurements of the solar irradiance in the 0.05 to 0.4 nm and 0.1 to 0.8 nm bands peaked at $1.89e-4$ W/m² and $4.97e-4$ W/m², respectively, during the February flare event. The measured soft X-ray enhancements started at approximately 00:41 UTC, reached a peak value at 00:49 UTC, and decreased by a factor of $1/\exp(2)$ at 01:19 UTC.

The Poker Flat Incoherent Scatter Radar (PFISR) was operating before, during, and after the flare event as part of the PFISR Ion-Neutral Interactions in the Thermosphere (PINOT) campaigns. It measured

significant electron density enhancements of up to approximately $2 \times 10^{11} \text{ m}^{-3}$ between 110 and 160 km altitude lasting 20 to 30 minutes. A more modest plasma density increase of approximately $2 \times 10^{10} \text{ m}^{-3}$ was observed between 90 and 110 km altitude. The enhanced plasma density was determined to be composed of mostly of O^{2+} and NO^{+} ions from ISR measurements and empirical models estimates. However, solar photons with wavelengths below 0.8 nm create additional ionization primarily at and below 110 km altitude, meaning that there likely was a significant enhancement in solar irradiance at wavelengths larger than the 0.8 nm wavelength upper limit of the GOES X-ray instrument.

Calculations from a physics-based self-consistent ionosphere model (SCIM) are presented for several case studies. Each case consists of a time-dependent calculation of the plasma density, composition, and temperature response to a simulated flare in the ionosphere above Poker Flat, Alaska. The first case assumes flare-enhanced solar irradiance is confined to wavelengths between 0.05 to 0.8 nm and shows that the calculated ionosphere response is not consistent with the ISR measurements. An estimated flare-enhanced solar ionizing spectrum with wavelengths above 0.8 nm is estimated by calculating the ionosphere response to subsequent flare cases. To bring the model-calculated plasma density profile to better agreement with the ISR-measured profiles, enhancements of irradiance at wavelengths between 0.8 to 2.0 nm of up to two orders of magnitude are required.

POLA-06 Observations of the high-velocity echoes from the polar E region with new Antarctic SuperDARN radars - by Forsythe, Victoriya V.

Status of First Author: Student IN poster competition, Undergraduate

Authors: V. V. Forsyth, R. A. Makarevich

Abstract: This study explores new opportunities associated with the recent deployment of several new High Frequency (HF) radars in Antarctica within the Super Dual Auroral Radar Network (SuperDARN). An interesting and a puzzling feature of observations with the McMurdo (MCM) and Dome C East (DCE) radars is that they regularly detect short-range E-region echoes with Doppler velocity close to or even significantly exceeding the nominal value for the ion-acoustic speed in the E region ($\sim 350 \text{ m/s}$). Such echoes are thought to be generated by the modified two-stream instability at angles between the wave propagation direction and the magnetic-field-perpendicular plane (aspect angles) that do not exceed 2° . However, the modeling results presented show that MCM and DCE radars have aspect angles ranging between 8° - 34° at typical E-region altitudes, even when the ionospheric refraction is taken into account. It is therefore a puzzling question why high-velocity echoes are observed at this very high aspect angle geometry. A unique experimental configuration of the MCM and DCE radars allows to observe the E-region irregularities simultaneously from two different directions using a pair of co-located beams. The Doppler velocity and echo occurrence analyzes showed that high-velocity echoes are not exceptionally rare events, with the occurrence trends showing a noticeable diurnal and seasonal pattern. A detailed comparison between the MCM and DCE velocities is presented for two 4-hour events that were observed on 13 February 2013 and 8 October 2013 as well as for the February and October monthly datasets. Possible reasons for the significant presence of high-velocity echoes in MCM and DCE datasets are discussed.

POLA-07 Ionospheric flow structures associated with auroral beading at the substorm auroral onset - by Gallardo Lacourt, Beatriz

Status of First Author: Student IN poster competition, Masters

Authors: Y. Nishimura, L. R. Lyons, J. M. Ruohoniemi, T. Motoba, E. Donovan, V. Angelopoulos, K. A. McWilliams, and N. Nishitani

Abstract: Auroral observations have shown that brightening at substorm auroral onset often consists of azimuthally propagating beads forming along a pre-existing arc. However, the ionospheric flow structure related to this wavy auroral structure has been poorly investigated. We investigated ionospheric flow patterns associated with auroral onset using line-of-sight flow observations from the Super Dual Auroral Radar Network (SuperDARN) and auroral images from the Time History of Events and Macroscale Interactions during Substorms (THEMIS) ground-based all-sky-imager (ASI) array. We have selected events where SuperDARN radars operated in a high temporal resolution THEMIS mode (6 seconds) along northward looking beams for radars, which is comparable to the time resolution of the imagers, providing a unique tool to detect properties of flows associated with the substorm onset instability. We have found very fast oscillating flows (~1000 m/s) that initiated simultaneously with the onset beads propagating across the THEMIS-mode beam meridian. 2-d radar measurements also show a wavy pattern in the azimuthal direction with a wavelength of ~78 km, which is close to the azimuthal separation of individual beads. We also used an imager and SuperDARN in Iceland and identified weak but significant azimuthal flow modulations associated with beads. These strong correlations (in time and space) between auroral beading and the fast ionospheric flows suggest that substorm onset instability in the inner plasma sheet is associated with intense flow shears. The flow shear is clockwise around auroral beads, consistent with converging electric fields associated with upward field-aligned currents in the shear center.

POLA-08 Negative AL index excursions and their influence on the high latitude F-region ion temperature at dusk - by Goodwin, Lindsay Victoria

Status of First Author: Student IN poster competition, PhD

Authors: Lindsay Victoria Goodwin, Jean-Pierre St. Maurice, Phil Richards, Mike Nicolls

Abstract: Using Poker Flat Incoherent Scatter Radar data from the International Polar Year, we observed unexpected short-lived ion temperature enhancements of a few 100K, or “Ti spikes”, being accompanied by sharp plasma density drops in the F region dusk plasmopause. These events would only occur when the radar was near the dusk boundary of the high latitude convection region and were often the largest ion temperature values recorded throughout the day. Even though the magnetic conditions at the time of these events were never very disturbed, the AL index would always go through a minimum of the order of -100nT at the time of the spikes. Given the altitude of the observations, ion frictional heating driven by large ion-neutral relative drifts had to be the cause of these temperature events. With this in mind, a plausible explanation for the spikes was that the negative AL excursions were associated not just with temporary intensifications in the electric field but also with an equatorward expansion of the convection pattern, leading to ions suddenly moving sunward in a region where the neutrals were still moving anti-sunward. This explanation is supported by the sharp decrease in plasma density seen near the ion temperature spikes. Another possibility, which might also agree with the plasma density data, is that weak substorms could have increased the electric fields at the plasmopause boundary, locally enhancing the ion frictional heating. These two hypotheses are being tested through modeling, larger magnetic and radar data sets, and specialized PINOT campaign experiments. Preliminary results from these studies are presented.

POLA-09 Reconstruction of Fine Scale Auroral Dynamics - by Hirsch, Michael

Status of First Author: Student IN poster competition, PhD

Authors: Michael Hirsch, Joshua Semeter, Matthew Zettergren, Hanna Dahlgren, Chhavi Goenka, Hassanali Akbari

Abstract: We present initial energy flux distribution inversion results from a 53 sample/second auroral tomography system implemented for auroral arc measurements in Alaska. We use a first-principles physics

forward model to invert brightness data into precipitating electron number flux. Initial results of our on-line auroral detection and characterization are shown.

We provide the first ever 20ms cadence tomographic analysis of the structure and motion in the aurora at sub-100m scales. Standard auroral tomography involves baselines of hundreds of kilometers as the peak auroral photometric volume emission rate (VER) is 100 km in altitude. To get sufficient signal-to-noise ratio, typical auroral observation systems have required sample times of seconds to minutes. However, it is well known that there is fine auroral structure of sub-100 m width with VER lifetimes on the order of 1 millisecond. Tomographic analysis of this fine structure requires camera baselines of 1-10 km. Intersite time synchronization of much better than 1ms is demonstrated. This short baseline combined with the practical requirement for earth-based cameras presents an ill-conditioned inverse problem due to the extreme viewing geometry. We discuss regularization schemes and potential resolutions for a number of issues that arise from the extreme geometry of a 3km ground baseline between Electron Multiplying CCD cameras.

POLA-10 Joule heating effects of small-scale structure and neutral winds in the high-latitude thermosphere/ionosphere - by Hurd, Lucas David

Status of First Author: Student IN poster competition, PhD

Authors: Hurd, L., M. F. Larsen

Abstract: Three barium chemical release rocket experiments have been investigated in order to study the effects of the neutral dynamics and small-scale electric field structure on the Joule heating in the polar latitudes during a variety of geomagnetic conditions. The ionized barium cloud technique provides time-varying measurements of the ion drift velocity within a spatially limited region, therefore yielding accurate small-scale electric field information that may be lost, e.g., when using probe techniques. A summary of results from the COPE 2 campaign in March 1987 at Sondre Stromfjord, Greenland, is presented, which also included trimethyl aluminum releases to measure the E-region neutral winds. In the context of the Joule heating problem, we have also revisited two campaigns from Andoya, Norway, in 1967 that measured strong electric field variations of up to 100 mV/m within only a few minutes, with peak magnitudes of up to 180 mV/m. For all of the experiments, there were significant changes in direction and magnitude of the electric field within small spatial regions and on fast time scales.

POLA-11 Fabry-Perot Interferometer Installed at Korean Jang Bogo Station (JBS), Antarctica - by Jee, Geonhwa

Status of First Author: Non-student, PhD

Authors: Jeong-Han Kim, Changsup Lee, Yong Ha Kim, Qian Wu

Abstract: Korean Antarctic Jang Bogo Station (JBS) has just started its operation in March, 2014, at Terra Nova Bay, Northern Victoria Land, Antarctica ($74^{\circ} 37.4' S$, $164^{\circ} 13.7' E$), which is located around the boundary region of the polar cap and the auroral region. This region is known for very strong coupling between neutrals and ions due to the plasma convection. In order to study this coupling and related physical processes, Korea Polar Research Institute (KOPRI) plans to install instruments such as Fabry-Perot Interferometer (FPI) and digital ionosonde in collaboration with High Altitude Observatory (HAO), NCAR and Cooperative Institute for Research in Environmental Sciences (CIRES), University of Colorado, respectively. We first installed FPI at JBS in March, 2014 to observe the neutral winds and temperature in the mesosphere and thermosphere and the digital ionosonde will be installed in the next summer season in January, 2015. In this talk, we introduce the FPI and the possible applications of the observed data.

POLA-12 Observations in the E-region ionosphere of kappa distribution functions associated with precipitating auroral electrons and discrete aurorae - by Kaeppler, Stephen R

Status of First Author: Non-student, PhD

Authors: Kaeppler, S. R.; Nicolls, M.; Stromme A.; Kletzing C. A.; Bounds S. R.

Abstract: Precipitating auroral electrons that cause discrete auroral arcs contain the imprint of the magnetospheric source region. Observations were obtained by on two payloads that comprised the Auroral Currents and Electrodynamics Structure (ACES) sounding rocket mission that successfully launched in January 2009 from Poker Flat Research Range, Alaska. The differential number flux observed by the electron detectors on the payload was fit to an accelerated Maxwellian or kappa distribution function [Evans, 1974] and parameters for the auroral source region were inferred from this model. The field-aligned precipitating electrons were fit better by a kappa distribution function for the equatorward side of a quasi-stable zonally extended auroral arc. These observations were made on the low altitude rocket payload at altitudes of approximately 130 km within the E-region ionosphere. The second half of the quasi-stable arc crossing and a second auroral crossing show the electrons were fit well by a Maxwellian distribution function or approximately Maxwellian kappa ($k > 10$) distribution function; these observations are additional confirmation of previous studies. A Monte Carlo technique is applied to the magnetospheric parameter estimates to quantify the uncertainty in the steady-state electron density, and the Hall and Pedersen conductivities over the auroral events. The properties of precipitating auroral electrons are investigated in the context of magnetospheric-ionospheric coupling and the effect precipitating electrons have on enhancing conductivities are quantified over a discrete aurora.

POLA-13 Thermosphere dynamics and composition changes - by Liu, Xianjing

Status of First Author: Non-student, PhD

Authors: Jeffrey P. Thayer, Aaron Ridley, Wenbin Wang, Alan Burns

Abstract: The helium module in the NCAR-TIEGCM was employed to study the thermosphere dynamics on the thermosphere neutral composition variation. Helium is an inert gas, which makes it an ideal thermosphere dynamics tracer. The effects of molecular diffusion, horizontal advection, vertical advection and eddy diffusion on the helium distribution were evaluated separately and quantitatively. The TIEGCM modeling results suggest that vertical advection is the main source for the helium enhancement in the winter hemisphere. Horizontal advection tends to eliminate the horizontal gradient of helium. And molecular diffusion acts to balance vertical advection to move helium back towards diffusive equilibrium. The contribution of the eddy diffusion on helium variation is small compared to the other three terms.

POLA-14 Correlation between Poynting flux and soft electron precipitation around the cusp region - by Sheng, Cheng

Status of First Author: Student IN poster competition, PhD

Authors: Cheng Sheng, Yue Deng, Yi-Jiun Su, Delores Knipp, Cheryl Y. Huang, Daniel Ober, and Rob Redmon

Abstract: Observations have revealed large Poynting flux and soft electron precipitation around the cusp region, which have strong impacts on the polar ionosphere/thermosphere. Simulations also confirmed that

Poynting flux and soft electron precipitation significantly change the neutral dynamics around the cusp. Commonly Poynting flux and soft electron precipitation are expected to happen at the same time and same location. Through analyzing DMSP observation data during storm times, the correlation between them is found to be more complex. In some cases the time and location of Poynting flux and soft electron precipitation are rather consistent, while are quite different in other cases. This result will improve our understanding of magnetosphere-ionosphere coupling, especially in the cusp region.

POLA-15 Time Evolution of Poynting Flux as Observed with the Swarm Satellites. -
by Patrick, Matthew Ryan

Status of First Author: Student IN poster competition, Masters

Authors: Matthew Patrick, David Knudsen, Johnathan Burchill, Claudia Stolle, Jan Rauberg

Abstract: The three Swarm satellites each carry a vector and scalar magnetometer as well as an Electric Field Instrument (EFI) that can be used to measure ion drift velocities. During the first months of the mission the satellites were in circular, polar orbits at an altitude of 490 kilometers, following each other in a pearls-on-a-string arrangement, separated by about one minute in time. This relatively close spatial formation allows comparisons to be done between electric field measurements on each satellite, revealing temporal changes of spatial structures. In this project we combine EFI data with vector magnetic field measurements to determine ionospheric Poynting Flux using each Swarm satellite. Cross correlation functions are calculated between measurements on each satellite and used to characterize the temporal and spatial scales of observed features. We find that on minute timescales, large-scale (~50-km-wide) regions of downward Poynting flux persist, but smaller-scale features evolve significantly.

Acknowledgements: The EFIs were developed and built by a consortium that includes the University of Calgary, the Swedish Institute for Space Physics in Uppsala, and COM DEV Canada. The Swarm EFI project is managed and funded by the European Space Agency with additional funding from the Canadian Space Agency.

POLA-16 Spatiotemporally resolved plasma and electric field structuring associated
with a sun-aligned arc over Resolute Bay - by Perry, Gareth W

Status of First Author: Student IN poster competition, PhD

Authors: G. W. Perry, H. Dahlgren, T. Sundberg, K. Hosokawa, M. J. Nicolls, J.-P. St.-Maurice, J. L. Semeter, and K. Shiokawa

Abstract: A case-study of a sun-aligned arc over Resolute Bay, Canada, that passed through the fields-of-view of radio and optical instruments is presented. The arc originated west of Resolute Bay at 5 UT (21:30 MLT), travelled eastward and passed through the fields-of-view of the Resolute Bay Incoherent Scatter Radar - North (RISR-N), the Optical Mesosphere and Thermosphere Imagers (OMTI) imager at Resolute Bay, and the Super Dual Auroral Radar Network (SuperDARN) instrument at Rankin Inlet, Canada. Using multipoint measurements from RISR-N to alleviate spatiotemporal ambiguities, the electrodynamic and plasma structuring of the arc and the surrounding area are investigated in detail. As the arc drifted into the RISR-N field-of-view, plasma flows which had been slow and disorganized were accelerated up to 2 km/s in an anti-sunward direction, in advance of the arc, and 1 km/s in the wake of the arc. Plasma flow shears were also observed — evidence of complex electric field structuring associated with the arc. Another notable feature of the event was a sun-aligned F-region density trough of non-local origin, located on the leading edge of the arc. The trough feature persisted on the leading edge of the arc throughout its transit

through the RISR-N field-of-view, implying significant plasma structuring by the arc. E-region plasma density enhancements collocated with the arc were also measured. Aggregating these details and other plasma parameter measurements from RISR-N, with the optical and HF radar information provided by OMTI and SuperDARN, respectively, the following questions are addressed: what is the nature and origin of the sun-aligned density trough on the leading edge of the arc; what was the generation mechanism of the arc and from where did it originate; why is the arc sun-aligned, and why does it drift in the dawn-to-dusk direction, despite being embedded in a predominately anti-sunward ExB velocity field?

POLA-17 Systematic assessment of the Ionosphere/Thermosphere models driven by different high latitude drivers - by Shim, Ja Soon

Status of First Author: Non-student

Authors: J. S. Shim, M. Kuznetsova, L. Rastaetter, M. Swindell, M. Codrescu, B. Emery, M. Foerster, B. Foster, T. Fuller-Rowell, A. J. Mannucci, A. Namgaladze, X. Pi, B. E. Prokhorov, A. Ridley, A. Coster, L. Goncharenko

Abstract: The CCMC (Community Coordinated Modeling Center) has developed tools that can be employed for easy driver swapping for Magnetosphere-Ionosphere coupling study. The tools allow us to convert ionosphere drivers from a variety of sources. For the high-latitude ionospheric electric potential, Weimer 2005, AMIE (assimilative mapping of ionospheric electrodynamics) and global magnetosphere models (e.g. Space Weather Modeling Framework, SWMF) can be used. In addition particle precipitation models can be converted between Fuller-Rowell & Evans, Roble & Ridley, and patterns derived from the ionosphere electrodynamics in the SWMF model. Using the tools, we studied the influence of high latitude drivers on Ionosphere/Thermosphere (IT). We obtained modeled IT parameters such as Total Electron Content (TEC), NmF2 and hmF2, and electron and neutral densities during the 2006 AGU storm event. We compared the modeled values with the observations for the 2006 AGU storm period and quantified the performance of the models using skill scores. Furthermore, the skill scores are obtained for three latitude regions (low, middle and high latitudes) in order to investigate latitudinal dependence of the models' performance. This study is supported by the CCMC at the Goddard Space Flight Center. Model outputs and observational data used for the study will be permanently posted at the CCMC website (<http://ccmc.gsfc.nasa.gov>) as a resource for the space science communities to use.

POLA-18 The Compact Echelle Spectrograph for Aeronomic Research (CESAR) - by Slanger, Tom

Status of First Author: Non-student

Authors: Tom G. Slanger, Daniel Matsiev, Jonas Hedin

Abstract: With support from the NSF Major Research Instrumentation (MRI) program the CESAR spectrograph has been completed and has been installed and operated at the Poker Flat Research Range since early November 2013. CESAR has been taking auroral and nightglow spectra since that time. Work has concentrated on studying the O₂ Atmospheric band system generated during aurorae. The ultimate spectral resolution of CESAR is ~16,000, but so far we have utilized $\lambda/d\lambda = 5000$, with data accumulation times on the order of 20 minutes, while covering a spectral range of 450-1000 nm. In general, auroral intensities have been low. Following earlier work [Sivjee et al., 1999] we have investigated auroral emission from the vibrational levels of the O₂(b) state, concentrating on levels $v=0-2$. The dominant source of auroral O₂(b) is the energy transfer interaction O(1D) + O₂, which generates mainly O₂(b, $v=1$) [Pejaković et al., 2014]. As the latter is strongly quenched to O₂(b, $v=0$) by O₂ and O(3P) [Pejaković et al., 2005a,b], its emission is concentrated at high altitudes, as evidenced by its high rotational temperature (up to 600 K). The O₂(b, $v=2$) level is best studied by means of the weak b-X 2-1 band, never previously used

for O2(b) investigations but free from contaminating auroral emissions. The O2(b, v=0) level is investigated by its normal (nightglow) probe - the 0-1 band - but the additional emission from auroral excitation is identified by the enhanced rotational temperature.

Pejaković, D.A. et al., J. Geophys. Res. 110, A03308, 2005a.

Pejaković, D.A., R.A. Copeland, T.G. Slanger, and K.S. Kalogerakis, Chem. Phys. Lett. 403, 372, 2005b.

Pejaković, D.A., R.A. Copeland, T.G. Slanger, and K.S. Kalogerakis, O2(b, v=0,1) Relative Yields in O(1D) + O2 Energy Transfer,

J. Geophys. Res. (accepted, 2014).

Sivjee, G.G., D. Shen, J.-H. Yee, and G. J. Romick, J. Geophys. Res. 104, 28003, 1999.

POLA-19 Index of Refraction Measurements in the Polar Cap Using the McMurdo Radar - by Spaleta, Jeffrey D

Status of First Author: Non-student, PhD

Authors: J. Spaleta, J. Klein, W. Bristow

Abstract: The McMurdo radar has the ability to operate at two independent radar frequencies simultaneously along a common beam direction. This capability makes it possible to extend the technique developed by Gillies et al. (2011) to provide an estimates of the index of refraction, ionospheric plasma density and line-of-sight velocity corrections from simultaneous dual velocity measurements. The McMurdo radar is well suited for this technique as it frequently sees a broad band of ionospheric scatter in its field of view that persists across a wide operational frequency range. During these periods of persistent scatter, it is possible to derive estimates for index of refraction and plasma density at the scattering region from the distribution of calculated values in the region. This poster includes analysis of McMurdo dual frequency operations from both 2012 and 2013.

POLA-20 Coordinated observations of polar cap flow channels by all-sky imagers and DMSP - by Wang, Boyi

Status of First Author: Student IN poster competition, PhD

Authors: Boyi Wang, Toshi Nishimura, Larry Lyons, Ying Zou

Abstract: Recent imager and radar observations in the nightside polar cap have shown evidence of localized flow channels propagating anti-sunward, and polar cap patches are often associated with such flow channels. It is crucial to understand how those polar cap flow channels and patches are created and propagate deep into the polar cap. In our study, we use all-sky imagers of the AGO network for dayside patch observations and DMSP for measuring density and velocity associated with those patches. Our conjunction events were found in the pre-noon sector due to the satellite orbits. We found that longitudinally narrow flow enhancements were well collocated with patches with substantially larger flow velocities than the weak large-scale background flows. The flow widths were similar to the patch widths (~390 km). Such associations were found common in statistics using (30) events in southern winter seasons of year 2007-2011, and we also get typical flow channel speed to be 776 m/sec, and width to be 354 km within our observation areas. Our conjunction events were found under -By-dominated IMF. It is consistent with the duskside convection cell extending toward dawn and giving a higher possibility of observations.

POLA-21 Localized polar cap flow enhancement evolution and tracing using airglow patches - by Zou, Ying

Status of First Author: Student NOT in poster competition, PhD

Authors: Ying Zou; Yukitoshi Nishimura; Larry R. Lyons; Kazuo Shiokawa, Eric F. Donovan; John Michael Ruohoniemi; Keisuke Hosokawa; Kathryn A. McWilliams; Nozomu Nishitani

Abstract: Previous radar observations have shown that polar cap flows are highly structured and that localized flow enhancements can lead to nightside auroral disturbances. While radar observations are limited to available echo regions, all-sky imagers (ASIs) allow tracing 2-d structures of polar cap emission over long distances. We utilized SuperDARN and the Resolute Bay ASI to study evolution of localized polar cap flows and airglow patches. We found that narrow flow enhancements were well collocated with patches with substantially larger velocities ($> \sim 200$ m/s) than the weak large-scale background flows. The flow azimuthal widths were similar to the patch widths. During the evolution across the polar cap, the flow directions and speeds were consistent with the patch propagation directions and speeds. These correspondences indicate that patches can optically trace localized flow enhancements reflecting the flow structure, speed and direction. Such associations were found common ($> 67\%$) in statistics, and the typical flow channel speed, propagation time, and width within our observation areas were 600 m/s, tens of minutes, and 200-300 km. By examining IMF dependence of the occurrence and properties of these flows, we found that they tended to be observed under By-dominated IMF. Flow speeds were large under oscillating IMF clock angles. Flow enhancements were usually observed as a channel elongated in the noon-midnight meridian and directed towards pre-midnight (post-midnight) for +By (-By). The potential drops across localized flow enhancements accounted for ~ 10 -40% of the cross polar cap potential, indicating their significant contribution to plasma transport in the polar cap.

POLA-22 High-latitude ionospheric drivers and their effects on wind patterns in the thermosphere - by Liuzzo, Lucas

Status of First Author: Student IN poster competition, Undergraduate

Authors: Liuzzo, L. R., A. J. Ridley, N. J. Perlongo, E. J. Mitchell, M. Conde, D. L. Hampton, W. A. Bristow, M. J. Nicolls

Abstract: Winds in the thermosphere are highly important for transporting mass, momentum, and energy over the globe. It has been moderately difficult to validate how well models reproduce the winds because of a lack of data. In the high latitude region, the ions and neutrals are strongly coupled when the aurora is present, whereas the coupling is less evident when there is no aurora. In this study, we investigate the ability of the Global Ionosphere Thermosphere Model (GITM) to simulate the meso-scale wind structure over Alaska during a substorm. Fourteen distinct numerical simulations of a substorm event that occurred between 02:00 and 17:00 universal time on November 24, 2012 have been performed. Using GITM, we are able to highlight both subtle and drastic differences in model results affected by various high-latitude ionospheric drivers. Distinct drivers considered include the Weimer potential patterns using IMF solar wind data coupled with the Fuller-Rowell and Evans auroral patterns, SuperDARN fitted potential pattern data, and changes in ionospheric currents measured by the Auroral Electrojet index. We also consider the effects of the boundary between the neutral wind dynamo calculation and the high-latitude imposed electric potential. Only the zonal component of the wind is compared, as this component is most strongly affected by ion-neutral coupling. Neutral wind velocities measured from Scanning Doppler Imager (SDI) instruments located at three locations in Alaska are then compared to GITM simulated winds for the runs studied. In addition, electron densities within GITM are compared with data from the Poker Flat Incoherent Scatter Radar instrument. We have found that differences in the driver used to model the substorm can lead to significantly disparate results among each individual run. This points to the need to

have accurate specifications of the electric potential and auroral precipitation if the wind patterns and behaviors are to be fully understood.

POLA-23 A statistical comparison of coupled thermosphere-ionosphere models - by Liuzzo, Lucas

Status of First Author: Student NOT in poster competition

Authors: Lucas Liuzzo

Abstract: The thermosphere-ionosphere system is a highly dynamic, non-linearly coupled interaction that fluctuates on a daily basis. Many models exist to attempt to quantify the relationship between the two atmospheric layers, and each approaches the problem differently. Because these models differ in the implementation of the equations that govern the dynamics of the thermosphere-ionosphere system, it is important to understand under which conditions each model performs best, and under which conditions each model may have limitations in accuracy. With this in consideration, this study examines the ability of two of the leading coupled thermosphere-ionosphere models in the community, TIE-GCM and GITM, to reproduce thermospheric and ionospheric quantities observed by the CHAMP satellite during times of differing geomagnetic activity. Neutral and electron densities are studied for three geomagnetic activity levels, ranging from high to minimal activity. Metrics used to quantify differences between the two models include root-mean-square error and prediction efficiency, and qualitative differences between a model and observed data is also considered. The metrics are separated into the high- mid- and low-latitude region to depict any latitudinal dependencies of the models during the various events. Despite solving for the same parameters, the models are shown to be highly dependent on the amount of activity level that occurs and can be significantly different from each other. In addition, in comparing previous statistical studies that use the models, a clear improvement is observed in the evolution of each model as thermospheric and ionospheric constituents during the differing levels of activity are solved.

Solar Terrestrial Interactions in the Upper Atmosphere

SOLA-01 Quantitative Assessment of the Ionosphere-Thermosphere Model Performances for the Orbit Averaged Storm Time Neutral Density along the CHAMP Satellite Track - by Kalafatoglu Eyiguler, Emine Ceren

Status of First Author: Student IN poster competition, PhD

Authors: Emine Ceren Kalafatoglu Eyiguler, Ja Soon Shim and Maria M. Kuznetsova

Abstract: Precise estimation of the thermospheric neutral density holds crucial importance for both research and operational point of view as neutral density is a key ingredient in the atmospheric drag acting on satellites at Low Earth Orbit. Though quiet time climatology is important for the calculation of the lifespan of a spacecraft at LEO, storm time changes can also increase the risk of collisions in the environment and can lead to a decrease in the satellite life time due to the increased atmospheric drag. Hence, we additionally require accurate predictions of the storm time neutral density change at the thermospheric altitudes. In this study, we use orbital averages of the modeled and observed neutral densities along the CHAMP satellite track for the community selected GEM-CEDAR storm events which consist of two minor, two moderate and two severe storms paving the way for quantification according to the activity levels. We use available ionosphere-thermosphere model runs performed by the CCMC (Community Coordinated Modeling Center) as well as results provided by modelers (e.g., NRLMSIS) for the investigation. We introduce methods to remove the quiet time climatology so that we can work with the

effects solely due to the geomagnetic storm. Taking into account their importance in the operations, the peak of the storm time neutral density, timing of the peak, storm time integrated density change and storm time average neutral density are selected as metrics for comparison. Furthermore, we use root mean square error (RMSE), sum of squared errors (SSE) and mean absolute error (MAE) to calculate the skill scores for the models. As a result, we find that quiet time climatology should be eliminated in order to better determine the modeled storm-time response, and skill scores should be calculated accordingly to quantify the storm time performances of the models.

SOLA-02 A quantitative analysis of solar X class flare effects on ionosonde and GPS TEC data - by Kim, Jeongheon

Status of First Author: Student IN poster competition, Masters

Authors: Jeongheon Kim, YongHa Kim, GeonHwa Jee

Abstract: It has been known that intense solar flux of EUV and X-ray during solar flares causes the ionosphere to change abruptly to the level of interfering radio communication. Now that more accurate observations of solar EUV and X-ray fluxes are available, we study the effect of solar flares on the ionosphere by comparing a physic-based model results with ionosonde and GPS TEC (total electron content) data. In order to simulate the effects of a solar flare, we have revised the SAMI2 model by including both photoionization of X-ray spectral range (below 50 Å) and photoelectron impact ionization. In this revision, we adopted X-ray fluxes measured by the TIMED/SEE instrument, and scale factors of photoionization cross sections of N₂, O₂, and O that account for photoelectron impact ionization effects. Since EUV peak fluxes from flares also contribute to ionization significantly, we adopted EUV fluxes measured by the SOHO/SEM. With the X-ray and EUV fluxes into with the revised SAMI2 model, we calculate peak densities of E and F₂ layers, and TEC for the largest 14 X class flare events over the last decade. After searching ionosonde data that contain critical frequencies of E and F₂ layers (foE, foF₂) with appropriate confidence levels, we found 13 and 25 of ionosonde data sets that have corresponding variations of foE and foF₂, respectively, to 9 X class flares. The information on GPS TEC was obtained from Liu et al. [2006] for 10 X-class flares among the selected 14 flares. We will present quantitative comparison of E and F₂ peak densities and TEC between the model results and measurements.

SOLA-03 Modeling Nitric Oxide in the Lower Thermosphere with measured Solar Soft X-ray Irradiance - by Lin, Ying-tsen

Status of First Author: Student IN poster competition, PhD

Authors: Cissi Y. Lin, Scott Bailey, Karthik Venkataramani

Abstract: Solar irradiance below 100 nm is the major driver for both neutral and ionized densities in the upper atmosphere though being a small fraction of total solar irradiance (TSI). Solar soft X-ray energy between 0.1 and 7 nm is absorbed mostly in the lower thermosphere between 100 and 150 km. Photoelectrons are created and initiate chains of photochemical reactions. One product, nitric oxide (NO), is a minor species in the thermosphere and an important indicator of energy balance. It also has the lowest ionization threshold so is the terminal ion in the ionospheric E-region. In this study, soft X-ray irradiance from the Solar Aspect Monitor (SAM) and EUV SpectroPhotometer (ESP) on the Solar Dynamic Observatory (SDO) is used to drive the NOx1D model during low, medium, and high solar activity levels. The effects of soft X-ray irradiance on thermospheric NO densities are compared.

SOLA-04 Forecasting the Impact of Equinoctial High-Speed Stream Structures on Thermospheric Responses - by McGranaghan, Ryan M.

Status of First Author: Student IN poster competition, Masters

Authors: Delores J. Knipp, Robert L. McPherron, Linda A. Hunt

Abstract: We examine thermospheric neutral density response to 172 solar wind high-speed streams (HSSs) and the associated stream interfaces during the equinox seasons of 2002-2008. HSSs produce prolonged enhancements in satellite drag. We find responses to two drivers: 1) the equinoctial Russell-McPherron (R-M) effect, which allows the azimuthal component of the interplanetary magnetic field (IMF) to project onto Earth's vertical dipole component; and 2) coronal streamer structures, which are extensions of the Sun's meso-scale magnetic field into space. Events for which the IMF projection is antiparallel to the dipole field are classified as "Effective-E", otherwise they are "Ineffective-I". Effective orientations enhance energy deposition and subsequently thermospheric density variations. The IMF polarities preceding and following stream interfaces at Earth produce events that are: Effective-Effective-EE; Ineffective-Ineffective-II; Ineffective-Effective-IE; and Effective-Ineffective-EI. These categories are additionally organized according to their coronal source structure: helmet streamers (HS-EI and HS-IE) and pseudo-streamers (PS-EE and PS-II). Approximately 65% of these combinations are HS-EI or HS-IE. The response to HS-IE structures is smoothly varying and long-lived, while the response to PS-EE structures is erratic, short-lived, and modulated by thermospheric preconditioning. We find significant distinguishable responses to these drivers in four geomagnetically sensitive observations: low-energy particle precipitation, proxied Joule heating, nitric oxide flux, and neutral density. Distinct signatures exist in neutral density response that can be anticipated days in advance based on currently available knowledge of on-disk coronal holes. Further, we show that the HS-IE events produce the largest neutral density disturbances, with the maximum IE perturbation density exceeding the maximum EI perturbation density by more than 30%.

**SOLA-05 Hemispheric asymmetries in the global aurora and IMF Bx -
by Reistad, Jone Peter**

Status of First Author: Student IN poster competition, Masters

Authors: J. P. Reistad, N. & Atilde;stgaard, K. M. Laundal, S. Haaland, P. Tenfjord, K. Snekvik, k. Oksavik, and S. E. Milan

Abstract: In the exploration of global-scale features of the Earth's aurora, little attention has been given to the radial component of the Interplanetary Magnetic Field (IMF). This study investigates the global auroral response in both hemispheres when the IMF is southward and lies in the xz-plane. We present a statistical study of the average auroral response in the 12-24 Magnetic Local Time (MLT) sector to an x-component in the IMF. Maps of auroral intensity in both hemispheres for two IMF Bx dominated conditions (+/- IMF Bx) are shown during periods of negative IMF Bz, small IMF By, and local winter. This is obtained by using global imaging from the Wideband Imaging Camera on the IMAGE satellite. The analysis indicates a significant asymmetry between the two IMF Bx dominated conditions in both hemispheres. In the Northern Hemisphere the aurora is brighter in the 15-19 MLT region during negative IMF Bx. In the Southern Hemisphere the aurora is brighter in the 16-20 MLT sector during positive IMF Bx. Our results are consistent with stronger Solar Wind (SW) dynamo efficiency in the Northern Hemisphere during negative IMF Bx and stronger SW dynamo efficiency in the Southern Hemisphere during positive IMF Bx. The difference in SW dynamo efficiency can be understood as an effect of hemispheric differences in magnetic tension forces on open field lines. This has earlier been suggested from case studies of simultaneous observations of the aurora in both hemispheres, but hitherto never been shown to have a general impact on global auroral brightness in both hemispheres. The observed asymmetries between the two IMF Bx cases are not large, however, the difference is significant with a 95 % confidence level. These results provide further confirmation that the asymmetric SW dynamo indeed can be responsible for hemispheric

asymmetries of the global aurora as suggested in earlier case studies. As the solar wind conditions examined in the study are rather common (37 % of the time) the accumulative effect of this small influence may be important in the total energy budget.

SOLA-06 Radiative cooling of the Thermosphere by infrared emissions from Nitric Oxide - by Venkataramani, Karthik

Status of First Author: Student IN poster competition, PhD

Authors: Karthik Venkataramani, Justin D. Yonker, Scott M. Bailey

Abstract: Thermal infrared emissions near $5.3\mu\text{m}$ from the vibrational bands of Nitric Oxide (NO) is an important source of radiative cooling in the thermosphere above 100 km. The vibrational levels of NO are populated by a combination of processes, the most important of which are inelastic collisions of NO with atomic oxygen and the exothermic reactions of ground state and excited atomic nitrogen with molecular oxygen. The former process is assumed to be the main contributor to radiative cooling during quiescent conditions, while the latter process gains significance at higher latitudes during active energy deposition. The purpose of this study is to quantify the relative contributions of these processes to radiative cooling in the thermosphere as a function of altitude, latitude and solar activity.

This is done by developing a steady state model for the NO vibrational levels, with level-specific production rates taken by introducing recent quantum-chemical results into the NO_x-1D model. The calculated emissions are then compared against data from the “Sounding of the Atmosphere using Broadband Emission Radiometry” (SABER) instrument on-board the TIMED satellite, which has been making measurements of the infrared radiative response of the mesosphere and thermosphere to solar inputs since 2002.

SOLA-07 Amplification of NO Production Rate in the Lower Thermosphere due to Catalysis of O₂⁺ - by Yonker, Justin David

Status of First Author: Non-student, PhD

Authors: Karthik Venkataramani, Cissi Ying-Tsen Lin, Scott M. Bailey

Abstract: An interesting coincidence occurs in the lower thermosphere in that the longest and shortest wavelengths of the solar EUV spectrum are absorbed at roughly the same altitude (100-110 km). The longest--the HI Lyman-Beta emission near 102.6 nm--leads immediately to O₂⁺ while the shortest--the solar x-ray irradiance shortward of about 20 nm--is, through a multi-step chemical cascade, a large source of NO. When both are present, O₂⁺ will steal an electron from the more easily ionized NO, converting it to NO⁺, and thereby destroying an NO. However, as is shown in this talk, this is actually the first step in a catalytic process, wherein the NO is largely recycled.

The importance of this catalytic process is demonstrated by considering the chemical reaction of the first excited electronic state of molecular nitrogen, N₂(A), with ground state atomic oxygen, N₂(A)+O->NO+N(2D), which in recent years has been found to be a key component of the net NO production rate. Including this reaction in a one-dimensional, photochemical model increases the midday, equatorial, NO production rate near 110 km by an average of 11%, with the catalytic cycle accounting for about 27% of this increase. Though the N₂(A)+O reaction is used to demonstrate the effect, the catalytic process is entirely general and serves to amplify any increase in the NO production rate in the presence of O₂⁺. However its efficiency is dependent on several environmental and quantum chemical factors and is shown to weaken with increasing altitude.

Akbari, Hassanali, 26
Andersen, Carl, 11
Anderson, Brian J., 25
Archer, William, 33

Burleigh, Meghan, 33
Bust, Gary Steven, 1

Cameron, Taylor, 26
Chen, Shih-Ping, 17
Chien, Shih Han, 31
Clayton, Robert, 34
Connor, Hyunju, 26
Cosgrove, Russell Bonner, 17
Crowley, Geoff, 18, 19

Deshpande, Kshitija Bharat, 20
Dhadly, Manbharat Singh, 11
Drob, Douglas Patrick, 24
Duly, Timothy, 28

Eltrass, Ahmed Said Hassan, 20
Emery, Barbara, 34
Emine Ceren, 44
Espinoza, Juan C, 4

Fallen, Christopher Thomas, 35
Fernandes, Philip, 12
Forsythe, Victoriya V., 35
Frissell, Nathaniel Anthony, 28

Gallardo Lacourt, Beatriz, 36
Gardner, Derek, 12
Geddes, George R, 12
Goenka, Chhavi, 13
Goodwin, Lindsay Victoria, 37

Hairston, Marc, 4
Harding, Brian J, 1
Hassan, Ehab, 5
Hawkins, Jessica, 24
Hew, Monica, 13
Hickey, Dustin A., 5
Hirsch, Michael, 37
Hong, Junseok, 5
Hsu, Chih Ting, 1
Hsu, Vicki, 6
Hurd, Lucas David, 38

Isham, Brett, 23

Jee, Geonhwa, 38

Kaeppler, Stephen R, 38
Kalafatoglu Eyiguler, 44
Kiene, Andrew Devon, 6
Kim, Jeongheon, 45
Kuyeng Ruiz, Karim M., 14

Lamarche, Leslie Jean, 21
Li, Zan, 27
Lin, Chi-Yen, 2
Lin, Fei-Fan, 21
Lin, Yen-Chieh, 29
Lin, Ying-tsen, 45
Liu, Xianjing, 39
Liuzzo, Lucas, 43
Lomidze, Levan, 29

Mabie, Justin J.E., 30
MacInnis, Rebecca, 7
Mangognia, Tony, 14
Mauk, Barry, 28
McGranaghan, Ryan M., 45
Mesquita, Rafael, 32
Moro, Juliano, 7

Nikoukar, Romina, 3
Nossal, Susan Marcelle, 25
Pacheco, Edgardo, 8

Patrick, Matthew Ryan, 39
Pawlowski, Dave, 3
Perez Ramirez, Freddy M., 30
Perry, Gareth W, 40
Pyle, Michelle Lynn, 14

Reimer, Ashton Seth, 15
Reistad, Jone Peter, 46
Rodrigues, Fabiano, 8

Sheng, Cheng, 39
Shim, Ja Soon, 41
Slanger, Tom, 41
Smith, Jessica Mae, 9
Sorbello, Robert Michael, 10
Sousa, Austin Patrick, 27
Spaleta, Jeffrey D, 42
Suarez Munoz, Daniel, 10
Sullivan, Catherine, 31
Sun, Weiwei, 15
Sun, Yang-Yi, 3
Swoboda, John P, 16

Tatton, Nicole, 16

Valladares, Cesar Enrique, 7
van der Meeren, Christer, 22
Venkataramani, Karthik, 47

Wang, Boyi, 42

Wang, Chien-Ya, 22

Yokoyama, Tatsuhiro, 23

Yonker, Justin David, 47

Zewdie, Gebreab Kidanu, 23

Zhu, Jie, 31

Zou, Ying, 42